

# Sequential Vector Parameter Estimation for Linear Models with Application to Distributed Systems

Yasin Yilmaz<sup>†</sup>, George V. Moustakides<sup>‡</sup>, and Xiaodong Wang<sup>†</sup>

## Abstract

Sequential estimation of a vector of linear regression coefficients is considered. In sequential estimation, the number of samples used for estimation is determined by the observed samples, hence is random, as opposed to fixed-sample-size estimation. Specifically, after receiving a new sample, we stop and estimate using the samples collected so far if a target accuracy level is reached; otherwise we continue to receive another sample. It is known that finding an optimal sequential estimator, which minimizes the average sample number for a given target accuracy level, is an intractable problem with a general stopping rule that depends on the complete observation history. By properly restricting the search space to stopping rules that depend on a specific subset of the complete observation history, we derive the optimal sequential estimators under two different formulations of the problem. In the first formulation, the (unconditional) covariance of the estimator is used to assess its accuracy, as a common practice. In the second formulation, the conditional covariance is used for the same purpose. Our analytical results show that the optimal stopping rule in the conditional formulation is a simple one-dimensional threshold rule for any number of parameters to be estimated. On the other hand, finding the optimal sequential estimator under the traditional unconditional formulation is not tractable even for a small number of parameters. We further propose, using level-triggered sampling, a computation-, and energy-efficient sequential estimator for the conditional problem in a wireless sensor network with strict energy constraints.

## Index Terms

Sequential estimation, vector parameter estimation, linear regression, distributed estimation, level-triggered sampling

<sup>†</sup>Electrical Engineering Department, Columbia University, New York, NY 10027.

<sup>‡</sup>Dept. of Electrical & Computer Engineering, University of Patras, 26500 Rion, Greece.

## I. INTRODUCTION

In this paper, we are interested in sequentially estimating a vector of parameters (i.e., regression coefficients)  $X \in \mathbb{R}^n$  at a random stopping time  $\mathcal{S}$  in the following linear (regression) model,

$$y_t = H_t^T X + w_t, \quad t \in \mathbb{N}, \quad (1)$$

where  $y_t \in \mathbb{R}$  is the observed sample,  $H_t \in \mathbb{R}^n$  is the vector of regressors and  $w_t \in \mathbb{R}$  is the additive noise. We consider the general case in which  $H_t$  is random and observed at time  $t$ , which covers the deterministic  $H_t$  case as a special case. This linear model is commonly used in many applications. For example, in system identification,  $X$  is the unknown system coefficients,  $H_t$  is the (random) input applied to the system, and  $y_t$  is the output at time  $t$ . Another popular example is the signal amplitude estimation in a communications channel, where  $X$  is the transmitted signal,  $y_t$  is the received signal,  $H_t$  is the (fading) channel gain (which is also estimated periodically using pilot signals), and  $w_t$  is the additive channel noise.

A sequential estimator  $(\mathcal{S}, \hat{X}_{\mathcal{S}})$ , as opposed to a traditional fixed-sample-size estimator, is equipped with a stopping rule which determines an appropriate time  $\mathcal{S}$  to stop taking samples based on the observed samples. Hence, the stopping time  $\mathcal{S}$  (i.e., the number of samples used in estimation) is a random variable. Endowed with a stopping mechanism, a sequential estimator is preferred to its fixed-sample-size counterpart especially when taking samples is costly, and thus we want to minimize the average sample number. Another advantage of sequential estimators is that they provide online estimates, whereas fixed-sample-size estimators produce offline estimates. More specifically, in sequential estimation, we keep refining our estimate as new samples arrive until no further refinement is needed (i.e., the accuracy of our estimator reaches a target level). On the other hand, in fixed-sample-size estimation, a single estimate is provided after observing a certain number of samples.

Distributed (e.g., cyberphysical) systems are currently a key area of research, with many emerging technologies such as wireless sensor networks, cognitive radio networks, smart grids, and networked control systems. Distributed estimation is a fundamental task that can be realized in such systems. Timing constraints are typical of distributed systems, which we can address with sequential estimators. However, the online nature of sequential estimation, in the ideal case, requires frequent high-rate data communications across the system, which becomes prohibitive for energy-constrained systems (e.g., a wireless sensor network with a large number of sensors). Thus, for such resource-constrained systems, designing resource-efficient distributed estimators is of utmost importance. On the other hand, fixed-sample-size estimators fail to satisfy both the timing and resource constraints in distributed systems since

a considerable amount of data communications simultaneously takes place at the deterministic estimation time, which may also cause congestion in the system [1].

### A. Outline

In the first part of the paper, for a restricted class of stopping rules that depend solely on the regressors  $\{H_t\}$  in (1), we derive the optimal sequential estimators, that minimize the average sample number for a given target accuracy level, under two different formulations of the problem. In the first formulation, we use the conditional covariance of the estimator given the regressors  $\{H_t\}$  to assess its accuracy, and show that the optimal stopping rule is a one-dimensional thresholding on the Fisher information, regardless of the dimension of the unknown parameter vector  $X$ . In the second formulation, following the common practice, we use the (unconditional) covariance of the estimator to assess its accuracy, and show that the complexity of the optimal stopping rule increases prohibitively with the dimension of  $X$ . Our analytical results demonstrate the usefulness of conditioning on ancillary statistics such as  $\{H_t\}$ . Although covariance is a generic accuracy measure, conditional covariance is preferred to it in the presence of an ancillary statistic that is independent of the unknown parameters [2].

Then, in the second part of the paper, from the optimal sequential estimator in the conditional problem, we develop a computationally efficient distributed sequential estimator that meets the timing and resource constraints in a wireless sensor network with stringent energy constraints. We achieve the energy efficiency via level-triggered sampling, a nonuniform sampling technique, and the computational efficiency through a simplification on the optimal estimator. Simulation results show that the simplified distributed estimator attains a very similar performance to those of the unsimplified distributed estimator and the optimal estimator when the regressors in  $H_t$  are uncorrelated. We also show in the simulation results that the performance gap between the simplified estimator and the unsimplified and optimal estimators increases with the correlation. Nevertheless, the simplified estimator achieves a good performance even in the correlated case.

We represent scalars with lower-case letters, vectors with upper-case letters and matrices with upper-case bold letters. In Section II, the sequential vector estimation problem is formulated. In Section III, we derive the optimal sequential estimators in the conditional and unconditional problems. We then propose a computationally efficient distributed sequential estimator in Section IV. Finally, the paper is concluded in Section V.

### B. Contributions

We contribute to both the optimal (centralized) and distributed sequential vector parameter estimation problems in linear models. In regard to centralized (i.e., non-distributed) sequential estimation, [1], [3] considered discrete-time observations, whereas [4] considered continuous-time observations. Moreover, [1], [4] proposed resource-efficient distributed sequential estimators using level-triggered sampling. Our contributions can be listed as follows.

- We analyze the general sequential vector parameter estimation problem under centralized and distributed settings, whereas [1], [3], [4] considered only the scalar parameter estimation problem.
- We derive the optimal sequential estimators under both the conditional and unconditional formulations of the vector parameter estimation problem, which proves the tractability and efficacy of the conditional formulation against the traditional unconditional formulation. Similar to our result, [2], [3], advocated using the conditional variance, instead of the unconditional variance, to assess the accuracy of an estimator in the presence of an ancillary statistic. However, [2] considered only fixed-sample-size estimation. Although [3] proposed a sequential estimator based on conditional variance, it did not provide any optimality result. Furthermore, [1] dealt with only the conditional formulation, and [4] analyzed the basic case of continuous-time observations, in which conditional and unconditional formulations coincide.
- In distributed estimation via level-triggered sampling, we propose to encode the random overshoot in each sample, which is due to discrete-time observations, in time, unlike [1], [5], which quantize the random overshoot, and [6], [7], which compute an average value for it.
- Instead of the direct implementation of level-triggered sampling for each dimension of the unknown parameter vector, which has a quadratic computational complexity in the number of dimensions, we develop a simplified distributed estimator based on level-triggered sampling with a linear computational complexity.

### C. Literature Review

The stopping capability of sequential estimators comes with the cost of sophisticated analysis. In most cases, finding an optimal sequential estimator that attains the sequential Cramér-Rao lower bound (CRLB) is not a tractable problem if the stopping time  $\mathcal{S}$  is adapted to the complete observation history [8]. Alternatively, in [3] and more recently in [1], [4], it was proposed to restrict  $\mathcal{S}$  to stopping times that are adapted to a specific subset of the complete observation history, which leads to simple solutions with alternative optimality. Note that this idea of using a restricted stopping time was first advocated in [3]

although without providing any optimality result. In the case of continuous-time observations, a sequential estimator with a restricted stopping time was shown to achieve the sequential version of the CRLB in [4]. In the discrete-time case, a similar sequential estimator was shown to achieve the conditional sequential CRLB in [1]. In this paper, with discrete-time observations and using a similar restricted stopping time we present the optimal sequential estimator for the more challenging unconditional problem. Moreover, we treat the vector parameter estimation problem, whereas only the scalar parameter estimation problem was considered in [1], [3], [4].

Distributed vector parameter estimation has been studied in a variety of papers, e.g., [9]–[18]. Among those [9], [10], [12]–[14] consider a wireless sensor network with a fusion center (FC), which computes a global estimator using local information received from sensors, whereas [15]–[18] consider ad hoc wireless sensor networks, where sensors in the absence of an FC compute their local estimators and communicate them through the network. Distributed estimation under both network topologies is reviewed in [11]. In [9], [11], [14], [15], [17], [18] a general nonlinear signal model is assumed. The majority of pertinent works in the literature, e.g., [9]–[16], studies fixed-sample-size estimation. There are a few works, such as [17], [18], that consider sequential distributed vector parameter estimation. Nevertheless, [17], [18] assume that sensors transmit real numbers, which obviously requires quantization in practice. In many applications quantization must be performed using a small number of bits due to the strict energy constraints on sensors. Recently, in a series of papers [1], [4]–[7] it was shown that level-triggered sampling, which is a non-uniform sampling method, meets those strict constraints by infrequently transmitting a single bit from sensors to the FC. Moreover, distributed schemes based on level-triggered sampling can significantly outperform their counterparts based on traditional uniform-in-time sampling [5]. Following the distributed schemes based on level-triggered sampling presented for scalar parameter estimation in [4] and [1] we propose in this paper a computationally efficient distributed scheme for vector parameter estimation.

## II. PROBLEM FORMULATION AND BACKGROUND

In (1), at each time  $t$ , we observe the sample  $y_t$  and the vector  $H_t$ , hence  $\{(y_p, H_p)\}_{p=1}^t$  are available. We assume  $\{w_t\}$  are i.i.d. with  $E[w_t] = 0$  and  $\text{Var}(w_t) = \sigma^2$ . We are interested in sequentially estimating  $X$ . The least squares (LS) estimator minimizes the sum of squared errors, i.e.,

$$\hat{X}_t = \arg \min_X \sum_{p=1}^t (y_p - H_p^T X)^2, \quad (2)$$

and is given by

$$\hat{X}_t = \left( \sum_{p=1}^t H_p H_p^T \right)^{-1} \sum_{p=1}^t H_p y_p = (\mathbf{H}_t^T \mathbf{H}_t)^{-1} \mathbf{H}_t^T Y_t, \quad (3)$$

where  $\mathbf{H}_t = [H_1, \dots, H_t]^T$  and  $Y_t = [y_1, \dots, y_t]^T$ .

Under the Gaussian noise,  $w_t \sim \mathcal{N}(0, \sigma^2)$ , the LS estimator coincides with the minimum variance unbiased estimator (MVUE), and achieves the CRLB, i.e.,  $\text{Cov}(\hat{X}_t | \mathbf{H}_t) = \text{CRLB}_t$ . To compute the CRLB we first write, given  $X$  and  $\mathbf{H}_t$ , the log-likelihood of the vector  $Y_t$  as

$$L_t = \log f(Y_t | X, \mathbf{H}_t) = - \sum_{p=1}^t \frac{(y_p - H_p^T X)^2}{2\sigma^2} - \frac{t}{2} \log(2\pi\sigma^2). \quad (4)$$

Then, we have

$$\text{CRLB}_t = \left( \mathbb{E} \left[ - \frac{\partial^2}{\partial X^2} L_t | \mathbf{H}_t \right] \right)^{-1} = \sigma^2 \mathbf{U}_t^{-1}, \quad (5)$$

where  $\mathbb{E} \left[ - \frac{\partial^2}{\partial X^2} L_t | \mathbf{H}_t \right]$  is the Fisher information matrix and  $\mathbf{U}_t \triangleq \mathbf{H}_t^T \mathbf{H}_t$  is a nonsingular matrix. Since  $\mathbb{E}[Y_t | \mathbf{H}_t] = \mathbf{H}_t X$  and  $\text{Cov}(Y_t | \mathbf{H}_t) = \sigma^2 \mathbf{I}$ , from (3) we have  $\mathbb{E}[\hat{X}_t | \mathbf{H}_t] = X$  and  $\text{Cov}(\hat{X}_t | \mathbf{H}_t) = \sigma^2 \mathbf{U}_t^{-1}$ , thus from (5)  $\text{Cov}(\hat{X}_t | \mathbf{H}_t) = \text{CRLB}_t$ . Note that the maximum likelihood (ML) estimator, that maximizes (4), coincides with the LS estimator in (3).

In general, the LS estimator is the best linear unbiased estimator (BLUE). In other words, any linear unbiased estimator of the form  $\mathbf{A}_t Y_t$  with  $\mathbf{A}_t \in \mathbb{R}^{n \times t}$ , where  $\mathbb{E}[\mathbf{A}_t Y_t | \mathbf{H}_t] = X$ , has a covariance no smaller than that of the LS estimator in (3), i.e.,  $\text{Cov}(\mathbf{A}_t Y_t | \mathbf{H}_t) \geq \sigma^2 \mathbf{U}_t^{-1}$  in the positive semidefinite sense. To see this result we write  $\mathbf{A}_t = (\mathbf{H}_t^T \mathbf{H}_t)^{-1} \mathbf{H}_t^T + \mathbf{B}_t$  for some  $\mathbf{B}_t \in \mathbb{R}^{n \times t}$ , and then  $\text{Cov}(\mathbf{A}_t Y_t | \mathbf{H}_t) = \sigma^2 \mathbf{U}_t^{-1} + \sigma^2 \mathbf{B}_t \mathbf{B}_t^T$ , where  $\mathbf{B}_t \mathbf{B}_t^T$  is a positive semidefinite matrix.

The recursive least squares (RLS) algorithm enables us to compute  $\hat{X}_t$  in a recursive way as follows

$$\begin{aligned} \hat{X}_t &= \hat{X}_{t-1} + K_t (y_t - H_t^T \hat{X}_{t-1}) \\ \text{where } K_t &= \frac{\mathbf{P}_{t-1} H_t}{1 + H_t^T \mathbf{P}_{t-1} H_t} \quad \text{and} \quad \mathbf{P}_t = \mathbf{P}_{t-1} - K_t H_t^T \mathbf{P}_{t-1}, \end{aligned} \quad (6)$$

where  $K_t \in \mathbb{R}^n$  is a gain vector and  $\mathbf{P}_t = \mathbf{U}_t^{-1}$ . While applying RLS we first initialize  $\hat{X}_0 = 0$  and  $\mathbf{P}_0 = \delta^{-1} \mathbf{I}$ , where 0 represents a zero vector and  $\delta$  is a small number, and then at each time  $t$  compute  $K_t$ ,  $\hat{X}_t$  and  $\mathbf{P}_t$  as in (6).

### III. OPTIMAL SEQUENTIAL ESTIMATORS

In this section we aim to find the optimal pair  $(\mathcal{T}, \hat{X}_{\mathcal{T}})$  of stopping time and estimator corresponding to the optimal sequential estimator. The stopping time for a sequential estimator is defined as the time it

first achieves a target accuracy level. We assess the accuracy of an estimator by using either its covariance matrix  $\text{Cov}(\hat{X}_t)$ , which averages also over  $\mathbf{H}_t$ , or conditional covariance matrix  $\text{Cov}(\hat{X}_t|\mathbf{H}_t)$ . Although traditionally the former is used in general, in the presence of an ancillary statistic whose distribution does not depend on the parameters to be estimated, such as  $\mathbf{H}_t$ , the latter was shown to be a better choice in [2] through asymptotic analysis. Specifically, the optimal sequential estimators can be formulated as the following constrained optimization problems,

$$\min_{\mathcal{T}, \hat{X}_{\mathcal{T}}} \mathbb{E}[\mathcal{T}|\mathbf{H}_{\mathcal{T}}] \quad \text{subject to} \quad f\left(\text{Cov}(\hat{X}_{\mathcal{T}}|\mathbf{H}_{\mathcal{T}})\right) \leq C, \quad (7)$$

$$\text{and} \quad \min_{\mathcal{T}, \hat{X}_{\mathcal{T}}} \mathbb{E}[\mathcal{T}] \quad \text{subject to} \quad f\left(\text{Cov}(\hat{X}_{\mathcal{T}})\right) \leq C, \quad (8)$$

under the conditional and unconditional setups, respectively, where  $f(\cdot)$  is a function from  $\mathbb{R}^{n \times n}$  to  $\mathbb{R}$  and  $C \in \mathbb{R}$  is the target accuracy level.

Note that the constraint in (7) is stricter than the one in (8) since it requires that  $\hat{X}_{\mathcal{T}}$  satisfies the target accuracy level for each realization of  $\mathbf{H}_{\mathcal{T}}$ , whereas in (8) it is sufficient that  $\hat{X}_{\mathcal{T}}$  satisfies the target accuracy level on average. In other words, in (8) even if for some realizations of  $\mathbf{H}_{\mathcal{T}}$  we have  $f\left(\text{Cov}(\hat{X}_{\mathcal{T}}|\mathbf{H}_{\mathcal{T}})\right) > C$ , we can still have  $f\left(\text{Cov}(\hat{X}_{\mathcal{T}})\right) \leq C$ . In fact, we can always have  $f\left(\text{Cov}(\hat{X}_{\mathcal{T}})\right) = C$  by using a probabilistic stopping rule such that we sometimes stop above  $C$ , i.e.,  $f\left(\text{Cov}(\hat{X}_{\mathcal{T}}|\mathbf{H}_{\mathcal{T}})\right) > C$ , and the rest of the time at or below  $C$ , i.e.,  $f\left(\text{Cov}(\hat{X}_{\mathcal{T}}|\mathbf{H}_{\mathcal{T}})\right) \leq C$ . On the other hand, in (7) we always have  $f\left(\text{Cov}(\hat{X}_{\mathcal{T}}|\mathbf{H}_{\mathcal{T}})\right) \leq C$ , and moreover since we observe discrete-time samples, in general we have  $f\left(\text{Cov}(\hat{X}_{\mathcal{T}}|\mathbf{H}_{\mathcal{T}})\right) < C$  for each realization of  $\mathbf{H}_{\mathcal{T}}$ . Hence, the optimal objective value  $\mathbb{E}[\mathcal{T}]$  in (8) will, in general, be smaller than the optimal objective value  $\mathbb{E}[\mathcal{T}|\mathbf{H}_{\mathcal{T}}]$  in (7). Note that on the other hand, if we observed continuous-time processes with continuous paths, then we could always have  $f\left(\text{Cov}(\hat{X}_{\mathcal{T}}|\mathbf{H}_{\mathcal{T}})\right) = C$  for each realization of  $\mathbf{H}_{\mathcal{T}}$ , and thus the optimal objective values of (7) and (8) would be the same.

The accuracy function  $f$  should be a monotonic function of the covariance matrices  $\text{Cov}(\hat{X}_{\mathcal{T}}|\mathbf{H}_{\mathcal{T}})$  and  $\text{Cov}(\hat{X}_{\mathcal{T}})$ , which are positive semi-definite, in order to make consistent accuracy assessments, e.g.,  $f(\text{Cov}(\hat{X}_{\mathcal{T}})) > f(\text{Cov}(\hat{X}_{\mathcal{S}}))$  for  $\mathcal{T} < \mathcal{S}$  since  $\text{Cov}(\hat{X}_{\mathcal{T}}) \succ \text{Cov}(\hat{X}_{\mathcal{S}})$  in the positive definite sense. Two popular and easy-to-compute choices are the trace  $\text{Tr}(\cdot)$ , which corresponds to the mean squared error (MSE), and the Frobenius norm  $\|\cdot\|_F$ . In the sequel we will next treat the two problems in (7) and (8) separately.

### A. The Optimal Conditional Sequential Estimator

Denote  $\{\mathcal{F}_t\}$  as the filtration that corresponds to the samples  $\{y_1, \dots, y_t\}$  where  $\mathcal{F}_t = \sigma\{y_1, \dots, y_t\}$  is the  $\sigma$ -algebra generated by the samples observed up to time  $t$  and  $\mathcal{F}_0$  is the trivial  $\sigma$ -algebra. Similarly we define the filtration  $\{\mathcal{H}_t\}$  where  $\mathcal{H}_t = \sigma\{H_1, \dots, H_t\}$ , i.e., the accumulated history related to the coefficient vectors, and  $\mathcal{H}_0$  is again the trivial  $\sigma$ -algebra. It is known that, in general, with discrete-time observations and an unrestricted stopping time, that is  $\{\mathcal{F}_t \cup \mathcal{H}_t\}$ -adapted, the sequential CRLB is not attainable under any noise distribution (Gaussian or non-Gaussian) except for the Bernoulli noise [8]. On the other hand, in the case of continuous-time observations with continuous paths the sequential CRLB is attainable by using an  $\{\mathcal{H}_t\}$ -adapted stopping time [4]. Moreover, with an  $\{\mathcal{H}_t\}$ -adapted stopping time, that depends only on  $\mathbf{H}_\mathcal{T}$ , the LS estimator attains the conditional sequential CRLB as we will show in the following Lemma. Hence, in this paper we restrict our attention to  $\{\mathcal{H}_t\}$ -adapted stopping times as in [1], [3], [4].

**Lemma 1.** *With a monotonic accuracy function  $f$  and an  $\{\mathcal{H}_t\}$ -adapted stopping time  $\mathcal{T}$  we can write*

$$f\left(\text{Cov}(\hat{X}_\mathcal{T}|\mathbf{H}_\mathcal{T})\right) \geq f\left(\sigma^2\mathbf{U}_\mathcal{T}^{-1}\right) \quad (9)$$

*for all unbiased estimators under Gaussian noise, and for all linear unbiased estimators under non-Gaussian noise, and the inequality in (9) holds with equality for the LS estimator.*

The proof of the Lemma is given in Appendix A. Since  $\mathcal{T}$  is  $\{\mathcal{H}_t\}$ -adapted, i.e., determined by  $\mathbf{H}_\mathcal{T}$ , we have  $\mathbb{E}[\mathcal{T}|\mathbf{H}_\mathcal{T}] = \mathcal{T}$ , and thus from (7) we want to find the first time that a member of our class of estimators (i.e., unbiased estimators under Gaussian noise and linear unbiased estimators under non-Gaussian noise) satisfies the constraint  $f\left(\text{Cov}(\hat{X}_\mathcal{T}|\mathbf{H}_\mathcal{T})\right) \leq C$ , as well as the estimator that attains this earliest stopping time. From Lemma 1 it is seen that the LS estimator achieves the earliest stopping time among its competitors. Hence, for the conditional problem the optimal pair of stopping time and estimator is  $(\mathcal{T}, \hat{X}_\mathcal{T})$  where  $\mathcal{T}$  is given by

$$\mathcal{T} = \min\{t \in \mathbb{N} : f\left(\sigma^2\mathbf{U}_t^{-1}\right) \leq C\}, \quad (10)$$

and from (3),

$$\hat{X}_\mathcal{T} = \mathbf{U}_\mathcal{T}^{-1}V_\mathcal{T}, \quad V_\mathcal{T} \triangleq \mathbf{H}_\mathcal{T}^T Y_\mathcal{T}, \quad (11)$$

which can be computed recursively as in (6). The recursive computation of  $\mathbf{U}_t^{-1} = \mathbf{P}_t$  in the test statistic in (10) is also given in (6). Note that for an accuracy function  $f$  such that  $f(\sigma^2\mathbf{U}_t^{-1}) = \sigma^2 f(\mathbf{U}_t^{-1})$ , e.g.,

$\text{Tr}(\cdot)$  and  $\|\cdot\|_F$ , we can use the following stopping time,

$$\mathcal{T} = \min\{t \in \mathbb{N} : f(\mathbf{U}_t^{-1}) \leq C'\}, \quad (12)$$

where  $C' = \frac{C}{\sigma^2}$  is the relative target accuracy with respect to the noise power. Hence, given  $C'$  we do not need to know the noise variance  $\sigma^2$  to run the test given by (12).

Note that  $\mathbf{U}_t = \mathbf{H}_t^T \mathbf{H}_t$  is a non-decreasing positive semi-definite matrix, i.e.,  $\mathbf{U}_t \succeq \mathbf{U}_{t-1}, \forall t$ , in the positive semi-definite sense. Thus, from the monotonicity of  $f$ , the test statistic  $f(\sigma^2 \mathbf{U}_t^{-1})$  is a non-increasing scalar function of time. Specifically, for accuracy functions  $\text{Tr}(\cdot)$  and  $\|\cdot\|_F$  we can show that if the minimum eigenvalue of  $\mathbf{U}_t$  tends to infinity as  $t \rightarrow \infty$ , then the stopping time is finite, i.e.,  $\mathcal{T} < \infty$ .

For the special case of scalar parameter estimation, we do not need a function  $f$  to assess the accuracy of the estimator since instead of a covariance matrix we now have a variance  $\frac{\sigma^2}{u_t}$ , where  $u_t = \sum_{p=1}^t h_p^2$  and  $h_t$  is the scaling coefficient in (1). Hence, from (12) the stopping time in the scalar case is given by

$$\mathcal{T} = \min \left\{ t \in \mathbb{N} : u_t \geq \frac{1}{C'} \right\}, \quad (13)$$

where  $\frac{u_t}{\sigma^2}$  is the Fisher information at time  $t$ . This result is in accordance with [1, Eq. (3)].

### B. The Optimal Unconditional Sequential Estimator

In this case we assume  $\{H_t\}$  is i.i.d.. From the constrained optimization problem in (8), using a Lagrange multiplier  $\lambda$  we obtain the following unconstrained optimization problem,

$$\min_{\mathcal{T}, \hat{X}_{\mathcal{T}}} \mathbb{E}[\mathcal{T}] + \lambda f\left(\text{Cov}(\hat{X}_{\mathcal{T}})\right). \quad (14)$$

We are again interested in  $\{\mathcal{H}_t\}$ -adapted stopping times to use the optimality property of the LS estimator in the sequential sense. For simplicity assume a linear accuracy function  $f$  so that  $f(\mathbb{E}[\cdot]) = \mathbb{E}[f(\cdot)]$ , e.g., the trace function  $\text{Tr}(\cdot)$ . Then, our constraint function becomes the sum of the individual variances, i.e.,  $\text{Tr}\left(\text{Cov}(\hat{X}_{\mathcal{T}})\right) = \sum_{i=1}^n \text{Var}(\hat{x}_{\mathcal{T}}^i)$ . Since  $\text{Tr}\left(\text{Cov}(\hat{X}_{\mathcal{T}})\right) = \text{Tr}\left(\mathbb{E}\left[\text{Cov}(\hat{X}_{\mathcal{T}}|\mathbf{H}_{\mathcal{T}})\right]\right) = \mathbb{E}\left[\text{Tr}\left(\text{Cov}(\hat{X}_{\mathcal{T}}|\mathbf{H}_{\mathcal{T}})\right)\right]$ , we rewrite (14) as

$$\min_{\mathcal{T}, \hat{X}_{\mathcal{T}}} \mathbb{E}\left[\mathcal{T} + \lambda \text{Tr}\left(\text{Cov}(\hat{X}_{\mathcal{T}}|\mathbf{H}_{\mathcal{T}})\right)\right], \quad (15)$$

where the expectation is with respect to  $\mathbf{H}_{\mathcal{T}}$ .

From Lemma 1, we have  $\text{Tr}\left(\text{Cov}(\hat{X}_{\mathcal{T}}|\mathbf{H}_{\mathcal{T}})\right) \geq \text{Tr}\left(\sigma^2 \mathbf{U}_{\mathcal{T}}^{-1}\right)$  where  $\sigma^2 \mathbf{U}_{\mathcal{T}}^{-1}$  is the covariance matrix of the LS estimator at time  $t$ . Note that  $\mathbf{U}_t/\sigma^2$  is the Fisher information matrix at time  $t$  [cf. (5)]. Using

the LS estimator we minimize the objective value in (15). Hence,  $\hat{X}_{\mathcal{T}}$  given in (11) [cf. (6) for recursive computation] is also the optimal estimator for the unconditional problem.

Now, to find the optimal stopping time we need to solve the following optimization problem,

$$\min_{\mathcal{T}} \mathbb{E} [\mathcal{T} + \lambda \text{Tr} (\sigma^2 \mathbf{U}_{\mathcal{T}}^{-1})], \quad (16)$$

which can be solved by using the *optimal stopping theory*. Writing (16) in the following alternative form

$$\min_{\mathcal{T}} \mathbb{E} \left[ \sum_{t=0}^{\mathcal{T}-1} 1 + \lambda \text{Tr} (\sigma^2 \mathbf{U}_{\mathcal{T}}^{-1}) \right], \quad (17)$$

we see that the term  $\sum_{t=0}^{\mathcal{T}-1} 1$  accounts for the cost of not stopping until time  $\mathcal{T}$  and the term  $\lambda \text{Tr} (\sigma^2 \mathbf{U}_{\mathcal{T}}^{-1})$  represents the cost of stopping at time  $\mathcal{T}$ . Note that  $\mathbf{U}_t = \mathbf{U}_{t-1} + H_t H_t^T$  and given  $\mathbf{U}_{t-1}$  the current state  $\mathbf{U}_t$  is (conditionally) independent of all previous states, hence  $\{\mathbf{U}_t\}$  is a Markov process. That is, in (17), the optimal stopping time for a Markov process is sought, which can be found by solving the following Bellman equation:

$$\mathcal{V}(\mathbf{U}) = \min \left\{ \underbrace{\lambda \text{Tr} (\sigma^2 \mathbf{U}^{-1})}_{F(\mathbf{U})}, \underbrace{1 + \mathbb{E}[\mathcal{V}(\mathbf{U} + H_1 H_1^T) | \mathbf{U}]}_{G(\mathbf{U})} \right\}, \quad (18)$$

where the expectation is with respect to  $H_1$  and  $\mathcal{V}$  is the optimal cost function [19]. The optimal cost function is obtained by iterating a sequence of functions  $\{\mathcal{V}_m\}$  where  $\mathcal{V}(\mathbf{U}) = \lim_{m \rightarrow \infty} \mathcal{V}_m(\mathbf{U})$  and

$$\mathcal{V}_m(\mathbf{U}) = \min \left\{ \lambda \text{Tr} (\sigma^2 \mathbf{U}^{-1}), 1 + \mathbb{E}[\mathcal{V}_{m-1}(\mathbf{U} + H_1 H_1^T) | \mathbf{U}] \right\}.$$

In the above optimal stopping theory, dynamic programming is used. Specifically, the original complex optimization problem in (16) is divided into simpler subproblems given by (18). At each time  $t$  we are faced with a subproblem consisting of a stopping cost  $F(\mathbf{U}_t) = \lambda \text{Tr} (\sigma^2 \mathbf{U}_t^{-1})$  and an expected sampling cost  $G(\mathbf{U}_t) = 1 + \mathbb{E}[\mathcal{V}(\mathbf{U}_{t+1}) | \mathbf{U}_t]$  to proceed to time  $t + 1$ . Since  $\{\mathbf{U}_t\}$  is a Markov process, and  $\{H_t\}$  is i.i.d., (18) is a general equation holding for all  $t$ . The optimal cost function  $\mathcal{V}(\mathbf{U}_t)$ , selecting the action with minimum cost (i.e., either continue or stop), determines the optimal policy to follow at each time  $t$ . That is, we stop the first time the stopping cost is smaller than the average cost of sampling, i.e.,

$$\mathcal{T} = \min \{t \in \mathbb{N} : \mathcal{V}(\mathbf{U}_t) = F(\mathbf{U}_t)\}.$$

We obviously need to analyze the structure of  $\mathcal{V}(\mathbf{U}_t)$ , i.e., the cost functions  $F(\mathbf{U}_t)$  and  $G(\mathbf{U}_t)$ , to find the optimal stopping time  $\mathcal{T}$ .

Note that  $\mathcal{V}$ , being a function of the symmetric matrix  $\mathbf{U} = [u_{ij}] \in \mathbb{R}^{n \times n}$ , is a function of  $\frac{n^2+n}{2}$  variables  $\{u_{ij} : i \leq j\}$ . Analyzing a multi-dimensional optimal cost function proves intractable, hence we

will first analyze the special case of scalar parameter estimation and then provide some numerical results for the two-dimensional vector case, demonstrating how intractable the higher dimensional problems are.

1) *Scalar case:* For the scalar case, from (18) we have the following one-dimensional optimal cost function,

$$\mathcal{V}(u) = \min \left\{ \frac{\lambda\sigma^2}{u}, 1 + \mathbb{E}[\mathcal{V}(u + h_1^2)] \right\}, \quad (19)$$

where the expectation is with respect to the scalar coefficient  $h_1$ . Specifically, at time  $t$  the optimal cost function is written as  $\mathcal{V}(u_t) = \min \left\{ \frac{\lambda\sigma^2}{u_t}, 1 + \mathbb{E}[\mathcal{V}(u_{t+1})] \right\}$ , where  $u_{t+1} = u_t + h_{t+1}^2$ . Writing  $\mathcal{V}$  as a function of  $z_t \triangleq 1/u_t$  we have  $\mathcal{V}(z_t) = \min \left\{ \lambda\sigma^2 z_t, 1 + \mathbb{E}[\mathcal{V}(z_{t+1})] \right\}$ , where  $z_{t+1} = \frac{z_t}{1+z_t h_{t+1}^2}$ , and thus in general

$$\mathcal{V}(z) = \min \left\{ \underbrace{\lambda\sigma^2 z}_{F(z)}, \underbrace{1 + \mathbb{E} \left[ \mathcal{V} \left( \frac{z}{1+z h_1^2} \right) \right]}_{G(z)} \right\}. \quad (20)$$

We need to analyze the cost functions  $F(z) = \lambda\sigma^2 z$  and  $G(z) = 1 + \mathbb{E} \left[ \mathcal{V} \left( \frac{z}{1+z h_1^2} \right) \right]$ . The former is a line, whereas the latter is, in general, a nonlinear function of  $z$ . We have the following lemma regarding the structure of  $\mathcal{V}(z)$  and  $G(z)$ . Its proof is given in the Appendix B.

**Lemma 2.** *The optimal cost  $\mathcal{V}$  and the expected sampling cost  $G$ , given in (20), are non-decreasing, concave and bounded functions of  $z$ .*

Following Lemma 2 the theorem below presents the stopping time for the scalar case of the unconditional problem.

**Theorem 1.** *The optimal stopping time for the scalar case of the unconditional problem in (8) with  $\text{Tr}(\cdot)$  as the accuracy function is given by*

$$\mathcal{T} = \min \left\{ t \in \mathbb{N} : u_t \geq \frac{1}{C''} \right\}, \quad (21)$$

where  $C''$  is selected so that  $\mathbb{E} \left[ \frac{\sigma^2}{u_{\mathcal{T}}} \right] = C$ , i.e., the variance of the estimator exactly hits the target accuracy level  $C$ .

*Proof:* The cost functions  $F(z)$  and  $G(z)$  are continuous functions as  $F$  is linear and  $G$  is concave. From (20) we have  $\mathcal{V}(0) = \min\{0, 1 + \mathcal{V}(0)\} = 0$ , hence  $G(0) = 1 + \mathcal{V}(0) = 1$ . Then, using Lemma 2 we illustrate  $F(z)$  and  $G(z)$  in Fig. 1. The optimal cost function  $\mathcal{V}(z)$ , being the minimum of  $F$  and  $G$  [cf. (20)], is also shown in Fig. 1. Note that as  $t$  increases  $z$  tends from infinity to zero. Hence, we continue until the stopping cost  $F(z_t)$  is lower than the expected sampling cost  $G(z_t)$ , i.e., until  $z_t \leq C''$ . The

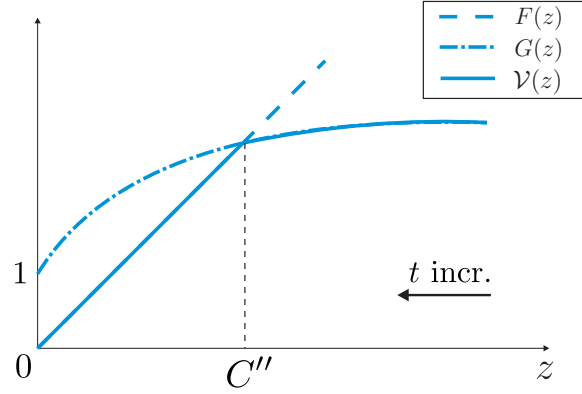


Fig. 1. The structures of the optimal cost function  $\mathcal{V}(z)$  and the cost functions  $F(z)$  and  $G(z)$ .

---

**Algorithm 1** The procedure to compute the threshold  $C''$  for given  $C$

---

- 1: Select  $C''$
  - 2: Estimate  $\mathcal{C} = \mathbb{E} \left[ \frac{\sigma^2}{u_{\mathcal{T}}} \right]$  through simulations, where  $u_t = \sum_{p=1}^t h_p^2$  and  $\mathcal{T} = \min \{t \in \mathbb{N} : u_t \geq \frac{1}{C'}\}$
  - 3: **if**  $\mathcal{C} = C$  **then**
  - 4: return  $C''$
  - 5: **else**
  - 6: **if**  $\mathcal{C} > C$  **then**
  - 7: Decrease  $C''$
  - 8: **else**
  - 9: Increase  $C''$
  - 10: **end if**
  - 11: Go to line 2
  - 12: **end if**
- 

threshold  $C''(\lambda) = \{z : F(\lambda, z) = G(z)\}$  is determined by the Lagrange multiplier  $\lambda$ , which is selected to satisfy the constraint  $\text{Var}(\hat{x}_{\mathcal{T}}) = \mathbb{E} \left[ \frac{\sigma^2}{u_{\mathcal{T}}} \right] = C$  [cf. (14)]. ■

Note that the optimal stopping time in (21) is of the same form as that in the scalar case of the conditional problem, where we have  $\mathcal{T} = \min \{t \in \mathbb{N} : u_t \geq \frac{1}{C'}\}$  from (13). In both conditional and unconditional problems the LS estimator

$$\hat{x}_{\mathcal{T}} = \frac{v_{\mathcal{T}}}{u_{\mathcal{T}}}$$

is the optimal estimator. The fundamental difference between the optimal stopping times in (13) and (21) is that the threshold in the conditional problem is written as  $C' = \frac{C}{\sigma^2}$ , hence known beforehand; whereas the threshold  $C''$  in the unconditional problem needs to be determined through offline simulations following the procedure in Algorithm 1, assuming that some training data  $\{h_t\}$  is available or the statistics

of  $h_t$  is known so that we can generate  $\{h_t\}$ . We also observe that  $C' \leq C''$ , hence the optimal objective value  $E[\mathcal{T}]$  of the unconditional problem is in general smaller than that of the conditional problem as noted earlier in this section. This is because the upper bound  $\sigma^2 C''$  on the conditional variance  $\frac{\sigma^2}{u_\tau}$  [cf. (21)] is also an upper bound for the variance  $E[\frac{\sigma^2}{u_\tau}] = C$ , and the threshold  $C'$  is given by  $C' = \frac{C}{\sigma^2}$ .

2) *Two-dimensional case:* We will next show that the multi-dimensional cases are intractable by providing some numerical results for the two-dimensional case. In the two-dimensional case, from (18) the optimal cost function is written as

$$\mathcal{V}(u_{11}, u_{12}, u_{22}) = \min \left\{ \lambda \sigma^2 \frac{u_{11} + u_{22}}{u_{11}u_{22} - u_{12}^2}, 1 + E \left[ \mathcal{V}(u_{11} + h_{1,1}^2, u_{12} + h_{1,1}h_{1,2}, u_{22} + h_{1,2}^2) \right] \right\},$$

$$\text{where } \mathbf{U} = \begin{bmatrix} u_{11} & u_{12} \\ u_{12} & u_{22} \end{bmatrix}, \quad \mathbf{H}_1 = \begin{bmatrix} h_{1,1} \\ h_{1,2} \end{bmatrix} \quad (22)$$

and the expectation is with respect to  $h_{1,1}$  and  $h_{1,2}$ . Changing variables we can write  $\mathcal{V}$  as a function of  $z_{11} \triangleq 1/u_{11}$ ,  $z_{22} \triangleq 1/u_{22}$  and  $\rho \triangleq u_{12}/\sqrt{u_{11}u_{22}}$ ,

$$\mathcal{V}(z_{11}, z_{22}, \rho) =$$

$$\min \left\{ \underbrace{\lambda \sigma^2 \frac{z_{11} + z_{22}}{1 - \rho^2}}_{F(z_{11}, z_{22}, \rho)}, 1 + E \left[ \underbrace{\mathcal{V} \left( \frac{z_{11}}{1 + z_{11}h_{1,1}^2}, \frac{z_{22}}{1 + z_{22}h_{1,2}^2}, \frac{\rho + h_{1,1}h_{1,2}\sqrt{z_{11}z_{22}}}{\sqrt{(1 + z_{11}h_{1,1}^2)(1 + z_{22}h_{1,2}^2)}} \right)}_{G(z_{11}, z_{22}, \rho)} \right] \right\}, \quad (23)$$

which can be iteratively computed as follows

$$\mathcal{V}_m(z_{11}, z_{22}, \rho) =$$

$$\min \left\{ \lambda \sigma^2 \frac{z_{11} + z_{22}}{1 - \rho^2}, 1 + E \left[ \mathcal{V}_{m-1} \left( \frac{z_{11}}{1 + z_{11}h_{1,1}^2}, \frac{z_{22}}{1 + z_{22}h_{1,2}^2}, \frac{\rho + h_{1,1}h_{1,2}\sqrt{z_{11}z_{22}}}{\sqrt{(1 + z_{11}h_{1,1}^2)(1 + z_{22}h_{1,2}^2)}} \right) \right] \right\}, \quad (24)$$

where  $\lim_{m \rightarrow \infty} \mathcal{V}_m = \mathcal{V}$ .

Note that  $\rho$  is the correlation coefficient, hence we have  $\rho \in [-1, 1]$ . Following the procedure in Algorithm 2 we numerically compute  $\mathcal{V}$  from (24) and find the boundary surface

$$\mathcal{S}(\lambda) = \{(z_{11}, z_{22}, \rho) : F(\lambda, z_{11}, z_{22}, \rho) = G(z_{11}, z_{22}, \rho)\},$$

that defines the stopping rule. In Algorithm 2, firstly the three-dimensional grid  $(n_1 dz, n_2 dz, n_3 dr)$ ,  $n_1, n_2 = 0, \dots, \frac{Rz}{dz}$ ,  $n_3 = -\frac{1}{dr}, \dots, \frac{1}{dr}$  is constructed. Then, in lines 5-7 the stopping cost  $F$  [cf. (23)] and in line 8 the first iteration of the optimal cost function  $\mathcal{V}_1$  with  $\mathcal{V}_0 = 0$  are computed over the grid. In lines 10-34, the optimal cost function  $\mathcal{V}$  is computed for each point in the grid by iterating  $\mathcal{V}_m$  [cf. (24)] until no significant change occurs between  $\mathcal{V}_m$  and  $\mathcal{V}_{m+1}$ . In each iteration, the double integral with respect

---

**Algorithm 2** The procedure to compute the boundary surface  $\mathcal{S}$  for given  $\lambda$

---

```

1: Set dz, Rz, dr, dh, Rh; Nz =  $\frac{Rz}{dz} + 1$ ; Nr =  $\frac{2}{dr} + 1$ ; Nh =  $\frac{2Rh}{dh} + 1$ 
2:  $z_1 = [0 : dz : Rz]$ ;  $z_2 = z_1$ ;  $\rho = [-1 : dr : 1]$  {all row vectors}
3:  $Z_1 = \mathbf{1}_{Nz} z_1$ ;  $Z_2 = Z_1^T$  { $\mathbf{1}_{Nz}$ : column vector of ones in  $\mathbb{R}^{Nz}$ }
4:  $h = [-Rh : dh : Rh]$ 
5: for  $i = 1 : Nr$  do
6:    $F(:, :, i) = \lambda \frac{Z_1 + Z_2}{1 - \rho(i)^2}$  {stopping cost over the 3D grid}
7: end for
8:  $\mathcal{V} = \min(F, 1)$  {start with  $\mathcal{V}_0 = 0$ }
9: dif =  $\infty$ ; Fr =  $\|\mathcal{V}\|_F$ 
10: while dif >  $\delta$  Fr { $\delta$ : a small threshold} do
11:   for  $i = 1 : Nz^2$  do
12:      $z_{11} = Z_1(i)$ ;  $z_{22} = Z_2(i)$  {linear indexing in matrices}
13:     for  $j = 1 : Nr$  do
14:        $G = 0$  {initialize continuing cost}
15:       for  $k = 1 : Nh$  do
16:          $h_1 = h(k)$  {scalar};  $h_2 = h$  {vector}
17:          $z'_{11} = z_{11}/(1 + z_{11}h_1^2)$  {scalar};  $Z'_{11} = z'_{11} \mathbf{1}_{Nh}$  {vector}
18:          $Z'_{22} = z_{22}/(1 + z_{22}h_2^2)$  {vector; dot denotes elementwise operation}
19:          $\rho' = [\rho(j) + h_1 h_2 \sqrt{z_{11} z_{22}}] / \sqrt{(1 + z_{11} h_1^2)(1 + z_{22} h_2^2)}$  {vector}
20:          $I_1 = Z'_{11}/dz + 1$ ;  $I_2 = Z'_{22}/dz + 1$ ;  $I_3 = (\rho' + 1)/dr + 1$  {fractional indices}
21:          $J^{8 \times Nh} =$  linear indices of 8 neighbor points using  $\lfloor I_n \rfloor, \lceil I_n \rceil, n = 1, 2, 3$ 
22:          $D_n = \lceil I_n \rceil - \lfloor I_n \rfloor$ ;  $\overline{D}_n = 1 - D_n, n = 1, 2, 3$  {distances to neighbor indices}
23:          $W^{8 \times Nh} =$  weights for neighbors as 8 multiplicative combinations of  $D_n, \overline{D}_n, n = 1, 2, 3$ 
24:          $V^{Nh \times 1} = \text{diag}(W^T \mathcal{V}(J))$  {average the neighbor  $\mathcal{V}$  values}
25:          $E^{1 \times Nh} = \frac{1}{2\pi} \exp(-\frac{1}{2}(h_1^2 + h_2^2)) dh^2$  {weights in the integral}
26:          $G = G + E V$  {update continuing cost}
27:       end for
28:        $\ell = i + (j - 1)Nz^2$  {linear index of the point the 3D grid}
29:        $\mathcal{V}'(\ell) = \min(F(\ell), 1 + G)$  {new optimal cost function}
30:     end for
31:   end for
32:   dif =  $\|\mathcal{V}' - \mathcal{V}\|_F$ ; Fr =  $\|\mathcal{V}\|_F$ 
33:    $\mathcal{V} = \mathcal{V}'$  {update the optimal cost function}
34: end while
35: Find the points where transition occurs between regions  $\mathcal{V} = F$  and  $\mathcal{V} \neq F$ , i.e.,  $\mathcal{S}$ .

```

---

to  $h_{1,1}$  and  $h_{1,2}$  corresponding to the expectation in (24) is computed in lines 15-27. While computing the integral, since the updated (future)  $(z_{11}, z_{22}, \rho)$  values, i.e., the arguments of  $\mathcal{V}_{m-1}$  in (24), in general may not correspond to a grid point, we average the  $\mathcal{V}_{m-1}$  values of eight neighboring grid points with appropriate weights in lines 21-24 to obtain the desired  $\mathcal{V}_{m-1}$  value.

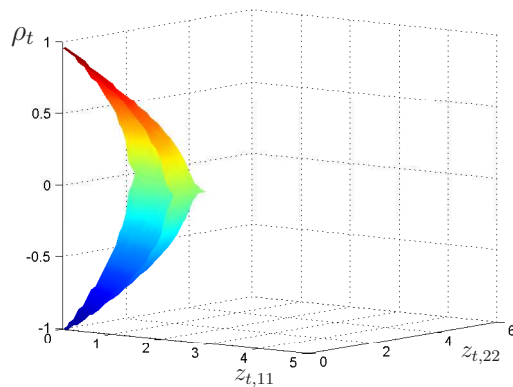


Fig. 2. The surface that defines the stopping rule for  $\lambda = 1$ ,  $\sigma^2 = 1$  and  $h_{1,1}, h_{1,2} \sim \mathcal{N}(0, 1)$  in the two-dimensional case.

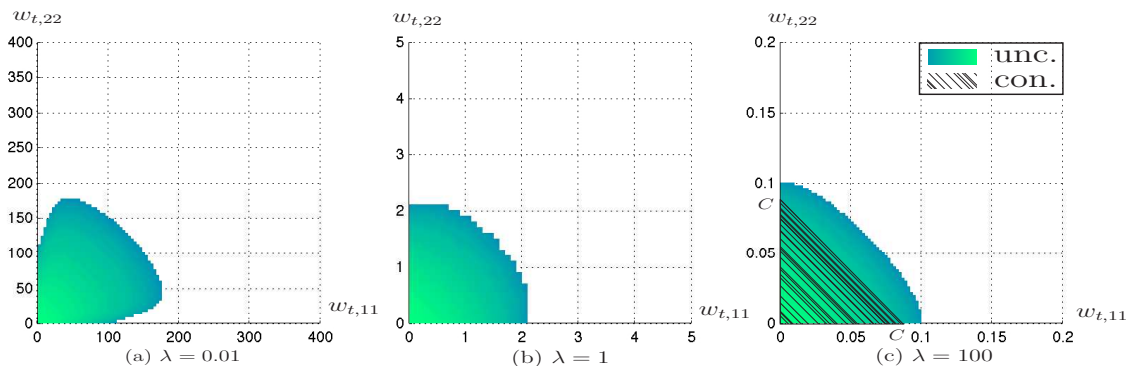


Fig. 3. The stopping regions for  $\rho_t = 0$ ,  $\sigma^2 = 1$  and  $h_{t,1}, h_{t,2} \sim \mathcal{N}(0, 1), \forall t$  in the unconditional problem with (a)  $\lambda = 0.01$ , (b)  $\lambda = 1$ , (c)  $\lambda = 100$ . That of the conditional problem is also shown in (c).

The results for  $\lambda \in \{0.01, 1, 100\}$ ,  $\sigma^2 = 1$  and  $h_{1,1}, h_{1,2} \sim \mathcal{N}(0, 1)$  are shown in Fig. 2 and Fig. 3. For  $\lambda = 1$ , the dome-shaped surface in Fig. 2 separates the stopping region from the continuing region. Outside the “dome”  $\mathcal{V} = G$ , hence we continue. As time progresses  $z_{t,11}$  and  $z_{t,22}$  decrease, so we move towards the “dome”. And whenever we are inside the “dome”, we stop, i.e.,  $\mathcal{V} = F$ . We obtain similar dome-shaped surfaces for different  $\lambda$  values. However, the cross-sections of the “domes” at specific  $\rho_t$  values differ significantly. In particular, we investigate the case of  $\rho_t = 0$ , where the scaling coefficients  $h_{t,1}$  and  $h_{t,2}$  are uncorrelated. For small values of  $\lambda$ , e.g.,  $\lambda = 0.01$ , the boundary that separates the stopping and the continuing regions is highly nonlinear as shown in Fig. 3(a). In Fig. 3(b) and 3(c), it is seen that the boundary tends to become more and more linear as  $\lambda$  increases.

Now let us explain the meaning of the  $\lambda$  value. Firstly, note from (23) that  $F$  and  $G$  are functions of

---

**Algorithm 3** The procedure to compute the boundary surface  $\mathcal{S}$ 


---

- 1: Select  $\lambda$
  - 2: Compute  $\mathcal{S}(\lambda)$  as in Algorithm 2
  - 3: Estimate  $\mathcal{C} = \mathbb{E} \left[ \sigma^2 \frac{z_{\mathcal{T},11} + z_{\mathcal{T},22}}{1 - \rho_{\mathcal{T}}^2} \right]$  through simulations, where  $z_{t,11} = 1/u_{t,11}$ ,  $z_{t,22} = 1/u_{t,22}$ ,  $\rho_t = u_{t,12}/\sqrt{u_{t,11}u_{t,22}}$  and  $\mathcal{T} = \min\{t \in \mathbb{N} : (z_{t,11}, z_{t,22}, \rho_t) \text{ is between } \mathcal{S} \text{ and the origin}\}$
  - 4: **if**  $\mathcal{C} = C$  **then**
  - 5: return  $\mathcal{S}$
  - 6: **else**
  - 7:   **if**  $\mathcal{C} > C$  **then**
  - 8:   Increase  $\lambda$
  - 9:   **else**
  - 10:   Decrease  $\lambda$
  - 11:   **end if**
  - 12: Go to line 2
  - 13: **end if**
- 

$z_{11}$ ,  $z_{22}$  for fixed  $\rho$ , and the boundary is the solution to  $F(\lambda, z_{11}, z_{22}) = G(z_{11}, z_{22})$ . When  $\lambda$  is small, the region where  $F < G$ , i.e., the stopping region, is large, hence we stop early as shown in Fig. 3(a)<sup>1</sup>. Conversely, for large  $\lambda$  the stopping region is small, hence the stopping time is large [cf. Fig. 3(c)]. In fact, the Lagrange multiplier  $\lambda$  is selected through simulations following the procedure in Algorithm 3 so that the constraint  $\text{Tr}(\mathbb{E}[\sigma^2 \mathbf{U}_{\mathcal{T}}^{-1}]) = \mathbb{E} \left[ \sigma^2 \frac{z_{\mathcal{T},11} + z_{\mathcal{T},22}}{1 - \rho_{\mathcal{T}}^2} \right] = C$  is satisfied. Note that line 2 of Algorithm 3 uses Algorithm 2 to compute the boundary surface  $\mathcal{S}$ .

In general, in the unconditional problem we need to numerically compute the stopping rule offline, i.e., the hypersurface that separates the stopping and the continuing regions, for a given target accuracy level  $C$ . This becomes a quite intractable task as the dimension  $n$  of the vector to be estimated increases since the computation of  $G$  in (23) involves computing an  $n$ -dimensional integral, which is then used to find the separating hypersurface in a  $\frac{n^2+n}{2}$ -dimensional space. On the other hand, in the conditional problem we have a simple stopping rule given in (12), which uses the target accuracy level  $\frac{C}{\sigma^2}$  as its threshold, hence known beforehand for any  $n$ . Specifically, in the two-dimensional case of the conditional problem the optimal stopping time is given by  $\mathcal{T} = \min \left\{ t \in \mathbb{N} : \frac{z_{t,11} + z_{t,22}}{1 - \rho_t^2} \leq \frac{C}{\sigma^2} \right\}$ , which is a function of  $z_{t,11} + z_{t,22}$  for fixed  $\rho_t$ . In Fig. 3(c), where  $\rho_t = 0$  and  $\sigma^2 = 1$ , the stopping region of the conditional problem, which is characterized by a line, is shown to be smaller than that of the unconditional problem due to the same reasoning in the scalar case.

<sup>1</sup>Note that the axis scales in Fig. 3(a) are on the order of hundreds and  $z_{t,11}$ ,  $z_{t,22}$  decrease as  $t$  increases.

#### IV. DISTRIBUTED SEQUENTIAL ESTIMATOR

In this section, we propose a computationally efficient scheme based on level-triggered sampling to implement the conditional sequential estimator in a distributed way. Consider a network of  $K$  distributed sensors and a fusion center (FC) which is responsible for computing the stopping time and the estimate. In practice, due to the stringent energy constraints, sensors should *infrequently* convey *low-rate* information to the FC, which is the main concern in the design of a distributed sequential estimator.

As in (1) each sensor  $k$  observes

$$y_t^k = (H_t^k)^T X + w_t^k, \quad t \in \mathbb{N}, \quad k = 1, \dots, K \quad (25)$$

as well as the coefficient vector  $H_t^k = [h_{t,1}^k, \dots, h_{t,n}^k]^T$  at time  $t$ , where  $\{w_t^k\}_{k,t}$ <sup>2</sup> are independent, zero-mean, i.e.,  $E[w_t^k] = 0$ ,  $\forall k, t$ , and  $\text{Var}(w_t^k) = \sigma_k^2$ ,  $\forall t$ . In other words, we allow for different noise variances at different sensors. Then, similar to (3) the weighted least squares (WLS) estimator

$$\hat{X}_t = \arg \min_X \sum_{k=1}^K \sum_{p=1}^t \frac{(y_p^k - (H_p^k)^T X)^2}{\sigma_k^2}$$

is given by

$$\hat{X}_t = \left( \sum_{k=1}^K \sum_{p=1}^t \frac{H_p^k (H_p^k)^T}{\sigma_k^2} \right)^{-1} \sum_{k=1}^K \sum_{p=1}^t \frac{H_p^k y_p^k}{\sigma_k^2} = \bar{U}_t^{-1} \bar{V}_t \quad (26)$$

where  $\bar{U}_t^k \triangleq \frac{1}{\sigma_k^2} \sum_{p=1}^t H_p^k (H_p^k)^T$ ,  $\bar{V}_t^k \triangleq \frac{1}{\sigma_k^2} \sum_{p=1}^t H_p^k y_p^k$ ,  $\bar{U}_t = \sum_{k=1}^K \bar{U}_t^k$  and  $\bar{V}_t = \sum_{k=1}^K \bar{V}_t^k$ . As before it can be shown that the WLS estimator  $\hat{X}_t$  in (26) is the BLUE under the general noise distributions. Moreover, in the Gaussian noise case, where  $w_t^k \sim \mathcal{N}(0, \sigma_k^2) \forall t$  for each  $k$ ,  $\hat{X}_t$  is also the MVUE. Note that  $\hat{X}_t$  in (26) coincides the ML estimator in the Gaussian case.

Following the steps in Section III-A it is straightforward to show that  $(\mathcal{T}, \hat{X}_{\mathcal{T}})$  is the optimal sequential estimator where

$$\mathcal{T} = \min \left\{ t \in \mathbb{N} : f(\bar{U}_t^{-1}) \leq C \right\}, \quad (27)$$

is the stopping time and the estimator  $\hat{X}_t$  is given in (26). Note that  $(\mathcal{T}, \hat{X}_{\mathcal{T}})$  is achievable only in the centralized case, where all local observations until time  $t$ , i.e.,  $\{(y_p^k, H_p^k)\}_{k,p}$ <sup>3</sup>, are available to the FC. Local processes  $\{\bar{U}_t^k\}_{k,t}$  and  $\{\bar{V}_t^k\}_{k,t}$  are used to compute the stopping time and the estimator as in (27) and (26), respectively. On the other hand, in a distributed system the FC can compute approximations  $\tilde{U}_t^k$  and  $\tilde{V}_t^k$  at each time  $t$ , and then use these approximations to compute the stopping time and the estimator as in (27) and (26), respectively.

<sup>2</sup>The subscripts  $k$  and  $t$  in the set notation denote  $k = 1, \dots, K$  and  $t \in \mathbb{N}$ .

<sup>3</sup>The subscript  $p$  in the set notation denotes  $p = 1, \dots, t$ .

### A. Key Approximations in Distributed Approach

Before proceeding to explain the proposed distributed scheme, we note that the RLS estimator is a special case of the Kalman filter, which is easily distributed through its inverse covariance form, namely the information filter. In the information filter, an  $n \times n$  matrix, namely the information matrix, and an  $n \times 1$  vector, namely the information vector, are used at each time, similar to  $\bar{\mathbf{U}}_t$  and  $\bar{\mathbf{V}}_t$  in the LS estimator, respectively. Distributed implementations of the information filter in the literature, e.g., [20], require the transmission of local information matrices and information vectors from sensors to the FC at each time  $t$ , which may not be practical, especially for large  $n$ , since it requires transmission of  $O(n^2)$  terms.

Considering  $\text{Tr}(\cdot)$  as the accuracy function  $f$  in (27), that is, assuming an MSE constraint, we propose to transmit only the  $n$  diagonal entries of  $\bar{\mathbf{U}}_t^k$  for each  $k$ , giving us a computationally tractable scheme with linear complexity, i.e.,  $O(n)$ , instead of quadratic complexity, i.e.,  $O(n^2)$ . Using the diagonal entries of  $\bar{\mathbf{U}}_t$  we define the diagonal matrix

$$\mathbf{D}_t \triangleq \text{diag}(d_{t,1}, \dots, d_{t,n})$$

$$\text{where } d_{t,i} = \sum_{k=1}^K \sum_{p=1}^t \frac{(h_{p,i}^k)^2}{\sigma_k^2}, \quad i = 1, \dots, n. \quad (28)$$

We further define the correlation matrix

$$\mathbf{R} = \begin{bmatrix} 1 & r_{12} & \cdots & r_{1n} \\ r_{12} & 1 & \cdots & r_{2n} \\ \vdots & \vdots & \ddots & \vdots \\ r_{1n} & r_{2n} & \cdots & 1 \end{bmatrix}, \quad (29)$$

$$\text{where } r_{ij} = \frac{\sum_{k=1}^K \frac{\mathbb{E}[h_{t,i}^k h_{t,j}^k]}{\sigma_k^2}}{\sqrt{\sum_{k=1}^K \frac{\mathbb{E}[(h_{t,i}^k)^2]}{\sigma_k^2} \sum_{k=1}^K \frac{\mathbb{E}[(h_{t,j}^k)^2]}{\sigma_k^2}}}, \quad i, j = 1, \dots, n.$$

**Proposition 1.** *For sufficiently large  $t$ , we can make the following approximations,*

$$\bar{\mathbf{U}}_t \cong \mathbf{D}_t^{1/2} \mathbf{R} \mathbf{D}_t^{1/2}$$

$$\text{and } \text{Tr}(\bar{\mathbf{U}}_t^{-1}) \cong \text{Tr}(\mathbf{D}_t^{-1} \mathbf{R}^{-1}). \quad (30)$$

The proof of Proposition 1 is provided in Appendix C. Then, assuming that the FC knows *a priori* the

correlation matrix  $\mathbf{R}$ , i.e.,  $\{E[h_{t,i}^k h_{t,j}^k]\}_{i,j,k}$ <sup>4</sup> and  $\{\sigma_k^2\}$  [cf. (29)], it can compute the approximations in (30) if sensors report their local processes  $\{\mathbf{D}_t^k\}_{k,t}$  to the FC, where  $\mathbf{D}_t = \sum_{k=1}^K \mathbf{D}_t^k$ . Note that each local process  $\{\mathbf{D}_t^k\}_t$  is  $n$ -dimensional, and its entries at time  $t$  are given by  $\{d_{t,i}^k = \sum_{p=1}^t \frac{(h_{p,i}^k)^2}{\sigma_k^2}\}_i$  [cf. (28)]. Hence, we propose that each sensor  $k$  sequentially reports the local processes  $\{\mathbf{D}_t^k\}_t$  and  $\{\bar{\mathbf{V}}_t^k\}_t$  to the FC, achieving linear complexity  $O(n)$ . On the other side, the FC, using the information received from sensors, computes the approximations  $\{\tilde{\mathbf{D}}_t\}$  and  $\{\tilde{\mathbf{V}}_t\}$ , which are then used to compute the stopping time

$$\tilde{\mathcal{T}} = \min \left\{ t \in \mathbb{N} : \text{Tr} \left( \tilde{\mathbf{U}}_t^{-1} \right) \leq \tilde{C} \right\}, \quad (31)$$

and the estimator

$$\tilde{\mathbf{X}}_{\tilde{\mathcal{T}}} = \tilde{\mathbf{U}}_{\tilde{\mathcal{T}}}^{-1} \tilde{\mathbf{V}}_{\tilde{\mathcal{T}}} \quad (32)$$

similar to (27) and (26), respectively. The approximations  $\text{Tr} \left( \tilde{\mathbf{U}}_t^{-1} \right)$  in (31) and  $\tilde{\mathbf{U}}_{\tilde{\mathcal{T}}}$  in (32) are computed using  $\tilde{\mathbf{D}}_t$  as in (30). The threshold  $\tilde{C}$  is selected through simulations to satisfy the constraint in (7) with equality, i.e.,  $\text{Tr} \left( \text{Cov}(\tilde{\mathbf{X}}_{\tilde{\mathcal{T}}} | \mathbf{H}_{\tilde{\mathcal{T}}}) \right) = C$ .

### B. Distributed Sequential Estimator Based on Level-triggered Sampling

Level-triggered sampling provides a very convenient way of information transmission in distributed systems as recently shown in [1], [4]–[7]. Methods based on level-triggered sampling, sending infrequently small number of bits, e.g., one bit, from sensors to the FC, enables highly accurate approximations and thus high performance schemes at the FC. They significantly outperform canonical sampling-and-quantizing methods which sample local processes using the conventional uniform-in-time sampling and send the quantized versions of samples to the FC [5]. On the other hand, level-triggered sampling, which is a non-uniform sampling technique, naturally outputs single-bit information. Moreover, the FC can effectively recover the samples of local processes by using these low-rate information from sensors.

All of the references above that propose schemes based on level-triggered sampling deal with one-dimensional, i.e., scalar, local processes. However, in our case  $\{\bar{\mathbf{V}}_t^k\}_t$  is  $n$ -dimensional and even worse

<sup>4</sup>The subscripts  $i$  and  $j$  in the set notation denote  $i = 1, \dots, n$  and  $j = i, \dots, n$ . In the special case where  $E[(h_{t,i}^k)^2] = E[(h_{t,i}^m)^2]$ ,  $k, m = 1, \dots, K$ ,  $i = 1, \dots, n$ , the correlation coefficients

$$\left\{ \xi_{ij}^k = \frac{E[h_{t,i}^k h_{t,j}^k]}{\sqrt{E[(h_{t,i}^k)^2] E[(h_{t,j}^k)^2]}} : i = 1, \dots, n-1, j = i+1, \dots, n \right\}_k$$

together with  $\{\sigma_k^2\}$  are sufficient statistics since  $r_{ij} = \frac{\sum_{k=1}^K \xi_{ij}^k / \sigma_k^2}{\sum_{k=1}^K 1 / \sigma_k^2}$  from (63).

$\{\bar{U}_t^k\}_t$  is  $\frac{n^2+n}{2}$ -dimensional <sup>5</sup> for each  $k$ . Applying a scheme that was proposed for one-dimensional processes in a straightforward fashion for each dimension, i.e., entry, of  $\bar{U}_t^k$  becomes cumbersome, especially when  $n$  is large. Hence, in this paper we propose to use the approximations introduced in the previous subsection, achieving linear complexity  $O(n)$ .

We will next describe the distributed scheme based on level-triggered sampling in which each sensor non-uniformly samples the local processes  $\{D_t^k\}_t$  and  $\{\bar{V}_t^k\}_t$ , transmits a single pulse for each sample to the FC, and the FC computes  $\{\tilde{D}_t\}$  and  $\{\tilde{V}_t\}$  using received information. Our scheme employs a novel algorithm to transmit a one-dimensional process, separately for each dimension of  $\{D_t^k\}_t$  and  $\{\bar{V}_t^k\}_t$ . In other words, our scheme at each sensor  $k$  consists of, in total,  $2n$  level-triggered samplers running in parallel.

1) *Sampling and Recovery of  $D_t^k$* : Each sensor  $k$  samples each entry  $d_{t,i}^k$  of  $D_t^k$  at a sequence of random times  $\{s_{m,i}^k\}_m$  <sup>6</sup> given by

$$s_{m,i}^k \triangleq \min \left\{ t \in \mathbb{N} : d_{t,i}^k - d_{s_{m-1,i}^k}^k \geq \Delta_i^k \right\}, \quad s_{0,i}^k = 0, \quad (33)$$

where  $d_{t,i}^k = \sum_{p=1}^t \frac{(h_{p,i}^k)^2}{\sigma_k^2}$ ,  $d_{0,i}^k = 0$  and  $\Delta_i^k > 0$  is a constant threshold that controls the average sampling interval. Note that the sampling times  $\{s_{m,i}^k\}_m$  in (33) are dynamically determined by the signal to be sampled, i.e., realizations of  $d_{t,i}^k$ . Hence, they are random, whereas sampling times in the conventional uniform-in-time sampling are deterministic with a certain period. According to the sampling rule in (33), a sample is taken whenever the signal level  $d_{t,i}^k$  increases by at least  $\Delta_i^k$  since the last sampling time. Note that  $d_{t,i}^k = \sum_{p=1}^t \frac{(h_{p,i}^k)^2}{\sigma_k^2}$  is non-decreasing in  $t$ .

At each sampling time  $s_{m,i}^k$ , sensor  $k$  transmits a single pulse to the FC at time  $t_{m,i}^k \triangleq s_{m,i}^k + \delta_{m,i}^k$ , indicating that  $d_{t,i}^k$  has increased by at least  $\Delta_i^k$  since the last sampling time  $s_{m-1,i}^k$ . The value of the transmitted pulse is not important since it only indicates  $d_{s_{m,i}^k}^k - d_{s_{m-1,i}^k}^k \geq \Delta_i^k$ . The delay  $\delta_{m,i}^k$  between the transmission time and the sampling time is used to linearly encode the overshoot

$$q_{m,i}^k \triangleq \left( d_{s_{m,i}^k}^k - d_{s_{m-1,i}^k}^k \right) - \Delta_i^k < \theta_d, \quad \forall k, m, i \quad (34)$$

and given by

$$\delta_{m,i}^k = \frac{q_{m,i}^k}{\phi_d} \in [0, 1), \quad (35)$$

where  $\phi_d^{-1}$  is the slope of the linear encoding function (cf. Fig. 4), known to sensors and the FC.

<sup>5</sup>This is because  $\bar{U}_t^k$  is symmetric.

<sup>6</sup>The subscript  $m$  in the set notation denotes  $m \in \mathbb{N}^+$ .

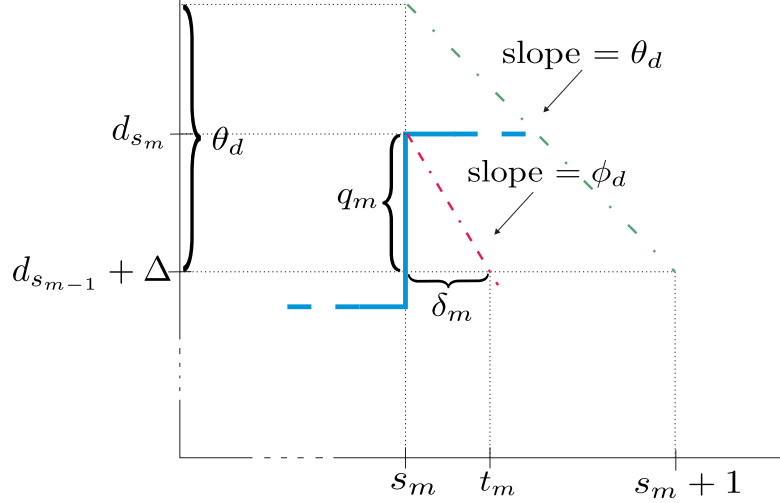


Fig. 4. Illustration of sampling time  $s_m$ , transmission time  $t_m$ , transmission delay  $\delta_m$  and overshoot  $q_m$ . We encode  $q_m = (d_{s_m} - d_{s_{m-1}}) - \Delta < \theta_d$  in  $\delta_m = t_m - s_m < 1$  using the slope  $\phi_d > \theta_d$ .

Assume a global clock, that is, the time index  $t \in \mathbb{N}$  is the same for all sensors and the FC, meaning that the FC knows the potential sampling times. Assume further ultra-wideband (UWB) channels between sensors and the FC, in which the FC can determine the time of flight of pulses transmitted from sensors. Then, FC can measure the transmission delay  $\delta_{m,i}^k$  if it is bounded by unit time, i.e.,  $\delta_{m,i}^k \in [0, 1)$ . To ensure this, from (35), we need to have  $\phi_d > q_{m,i}^k, \forall k, m, i$ . Assuming a bound for overshoots, i.e.,  $q_{m,i}^k < \theta_d, \forall k, m, i$ , we can achieve this by setting  $\phi_d > \theta_d$ <sup>7</sup>. Consequently, the FC can uniquely decode the overshoot by computing  $q_{m,i}^k = \phi_d \delta_{m,i}^k$  (cf. Fig. 4), using which it can also find the increment occurred in  $d_{t,i}^k$  during the interval  $(s_{m-1,i}^k, s_{m,i}^k]$  as  $d_{s_{m,i},i}^k - d_{s_{m-1,i},i}^k = \Delta_i^k + q_{m,i}^k$  from (34). It is then possible to reach the signal level  $d_{s_{m,i},i}^k$  by accumulating the increments occurred until the  $m$ th sampling time, i.e.,

$$d_{s_{m,i},i}^k = \sum_{\ell=1}^m (\Delta_i^k + q_{\ell,i}^k) = m\Delta_i^k + \sum_{\ell=1}^m q_{\ell,i}^k. \quad (36)$$

Using  $\{d_{s_{m,i},i}^k\}_m$  the FC computes the staircase approximation  $\tilde{d}_{t,i}^k$  as

$$\tilde{d}_{t,i}^k = d_{s_{m,i},i}^k, \quad t \in [t_{m,i}^k, t_{m+1,i}^k), \quad (37)$$

which is updated when a new pulse is received from sensor  $k$ , otherwise kept constant. Such approximate

<sup>7</sup>In fact, by setting the slope  $\phi_d$  arbitrarily large we can make the transmission delay arbitrarily small.

local signals of different sensors are next combined to obtain the approximate global signal  $\tilde{d}_{t,i}$  as

$$\tilde{d}_{t,i} = \sum_{k=1}^K \tilde{d}_{t,i}^k. \quad (38)$$

In practice, when the  $m$ th pulse in the global order regarding dimension  $i$  is received from sensor  $k_m$  at time  $t_{m,i}$ , instead of computing (36)–(38) the FC only updates  $\tilde{d}_{t,i}$  as

$$\tilde{d}_{t_{m,i},i} = \tilde{d}_{t_{m-1,i},i} + \Delta_i^{k_m} + q_{m,i}, \quad \tilde{d}_{0,i} = \epsilon, \quad (39)$$

and keeps it constant when no pulse arrives. We initialize  $\tilde{d}_{t,i}$  to a small constant  $\epsilon$  to prevent dividing by zero while computing the test statistic [cf. (40)]. Note that in general  $\tilde{d}_{t_{m,i},i} \neq d_{s_{m,i},i}$  unlike (37) since all sensors do not necessarily sample and transmit at the same time. The approximations  $\{\tilde{d}_{t,i}\}_i$  form  $\tilde{\mathbf{D}}_t = \text{diag}(\tilde{d}_{t,1}, \dots, \tilde{d}_{t,n})$ , which is used in (31) and (32) to compute the stopping time and the estimator, respectively. Note that to determine the stopping time as in (31) we need to compute  $\text{Tr}(\tilde{\mathbf{U}}_t^{-1})$  using (30) at times  $\{t_m\}$  when a pulse is received from any sensor regarding any dimension. Fortunately, when the  $m$ th pulse in the global order is received from sensor  $k_m$  at time  $t_m$  regarding dimension  $i_m$  we can compute  $\text{Tr}(\tilde{\mathbf{U}}_{t_m}^{-1})$  recursively as follows

$$\text{Tr}(\tilde{\mathbf{U}}_{t_m}^{-1}) = \text{Tr}(\tilde{\mathbf{U}}_{t_{m-1}}^{-1}) - \frac{\kappa_{i_m}(\Delta_{i_m}^{k_m} + q_m)}{\tilde{d}_{t_m,i_m} \tilde{d}_{t_{m-1},i_m}}, \quad \text{Tr}(\tilde{\mathbf{U}}_0^{-1}) = \sum_{i=1}^n \frac{\kappa_i}{\epsilon}, \quad (40)$$

where  $\kappa_i$  is the  $i$ th diagonal element of the inverse correlation matrix  $\mathbf{R}^{-1}$ , known to the FC. In (40) pulse arrival times are assumed to be distinct for the sake of simplicity. In case multiple pulses arrive at the same time, the update rule will be similar to (40) except that it will consider all new arrivals together.

2) *Sampling and Recovery of  $\bar{\mathbf{V}}_t^k$* : Similar to (33) each sensor  $k$  samples each entry  $\bar{v}_{t,i}^k$  of  $\bar{\mathbf{V}}_t^k$  at a sequence of random times  $\{\alpha_{m,i}^k\}_m$  written as

$$\alpha_{m,i}^k \triangleq \min \left\{ t \in \mathbb{N} : |\bar{v}_{t,i}^k - \bar{v}_{\alpha_{m-1,i}^k}^k| \geq \gamma_i^k \right\}, \quad \alpha_{0,i}^k = 0, \quad (41)$$

where  $\bar{v}_{t,i}^k = \sum_{p=1}^t \frac{h_{p,i}^k y_p^k}{\sigma_k^2}$  and  $\gamma_i^k$  is a constant threshold, available to both sensor  $k$  and the FC. It has been shown in [5, Section IV-B] that  $\gamma_i^k$  is determined by

$$\gamma_i^k \tanh(\gamma_i^k/2) = T \sum_{k=1}^K \frac{\mathbb{E}[\bar{v}_{t,i}^k]}{K}$$

to ensure the average sampling interval  $T$ . Since  $\bar{v}_{t,i}^k$  is neither increasing nor decreasing, we use two thresholds  $\gamma_i^k$  and  $-\gamma_i^k$  in the sampling rule given in (41). Specifically, a sample is taken whenever  $\bar{v}_{t,i}^k$  increases or decreases by at least  $\gamma_i^k$  since the last sampling time. Then, sensor  $k$  at time  $p_{m,i}^k \triangleq \alpha_{m,i}^k + \beta_{m,i}^k$

---

**Algorithm 4** The level-triggered sampling procedure at the  $k$ th sensor for the  $i$ th dimension
 

---

```

1: Initialization:  $t \leftarrow 0$ ,  $m \leftarrow 0$ ,  $\ell \leftarrow 0$ ,  $\chi \leftarrow 0$ ,  $\psi \leftarrow 0$ 
2: while  $\chi < \Delta_i^k$  and  $\psi \in (-\gamma_i^k, \gamma_i^k)$  do
3:    $t \leftarrow t + 1$ 
4:    $\chi \leftarrow \chi + \frac{(h_{t,i}^k)^2}{\sigma_k^2}$ 
5:    $\psi \leftarrow \psi + \frac{h_{t,i}^k y_t^k}{\sigma_k^2}$ 
6: end while
7: if  $\chi \geq \Delta_i^k$  {sample  $d_{t,i}^k$ } then
8:    $m \leftarrow m + 1$ 
9:    $s_{m,i}^k = t$ 
10:  Send a pulse to the fusion center through channel  $\text{ch}_{k,i}^d$  at time instant  $t_{m,i}^k = s_{m,i}^k + \frac{\chi - \Delta_i^k}{\phi_d}$ 
11:   $\chi \leftarrow 0$ 
12: end if
13: if  $\psi \notin (-\gamma_i^k, \gamma_i^k)$  {sample  $\bar{v}_{t,i}^k$ } then
14:    $\ell \leftarrow \ell + 1$ 
15:    $\alpha_{\ell,i}^k = t$ 
16:   Send  $b_{\ell,i}^k = \text{sign}(\psi)$  to the fusion center through channel  $\text{ch}_{k,i}^v$  at time instant  $p_{\ell,i}^k = \alpha_{\ell,i}^k + \frac{|\psi| - \gamma_i^k}{\phi_v}$ 
17:    $\psi \leftarrow 0$ 
18: end if
19: Stop if the fusion center instructs so; otherwise go to line 2.

```

---

transmits a single pulse  $b_{m,i}^k$  to the FC, indicating whether  $\bar{v}_{t,i}^k$  has changed by at least  $\gamma_i^k$  or  $-\gamma_i^k$  since the last sampling time  $\alpha_{m-1,i}^k$ . We can simply write  $b_{m,i}^k$  as

$$b_{m,i}^k = \text{sign}(\bar{v}_{\alpha_{m,i}^k,i}^k - \bar{v}_{\alpha_{m-1,i}^k,i}^k), \quad (42)$$

where  $b_{m,i}^k = 1$  implies that  $\bar{v}_{\alpha_{m,i}^k,i}^k - \bar{v}_{\alpha_{m-1,i}^k,i}^k \geq \gamma_i^k$  and  $b_{m,i}^k = -1$  indicates that  $\bar{v}_{\alpha_{m,i}^k,i}^k - \bar{v}_{\alpha_{m-1,i}^k,i}^k \leq -\gamma_i^k$ . The overshoot  $\eta_{m,i}^k \triangleq |\bar{v}_{\alpha_{m,i}^k,i}^k - \bar{v}_{\alpha_{m-1,i}^k,i}^k| - \gamma_i^k$  is linearly encoded in the transmission delay as before. Similar to (35) the transmission delay is written as  $\beta_{m,i}^k = \frac{\eta_{m,i}^k}{\phi_v}$ , where  $\phi_v^{-1}$  is the slope of the encoding function, available to sensors and the FC. Assume again that (i) there exists a global clock among sensors and the FC, (ii) the FC determines channel delay (i.e., time of flight), and (iii) overshoots are bounded by a constant, i.e.,  $\eta_{m,i}^k < \theta_v$ ,  $\forall k, m, i$ , and we set  $\phi_v > \theta_v$ . With these assumptions we ensure that the FC can measure the transmission delay  $\beta_{m,i}^k$ , and accordingly decode the overshoot as  $\eta_{m,i}^k = \phi_v \beta_{m,i}^k$ . Then, upon receiving the  $m$ th pulse  $b_{m,i}^k$  regarding dimension  $i$  from sensor  $k_m$  at time  $p_{m,i}^k$  the FC performs the following update,

$$\tilde{v}_{p_{m,i}^k,i} = \tilde{v}_{p_{m-1,i}^k,i} + b_{m,i}^k (\gamma_i^{k_m} + \eta_{m,i}^k), \quad (43)$$

---

**Algorithm 5** The sequential estimation procedure at the fusion center
 

---

- 1: Initialization:  $\text{Tr} \leftarrow \sum_{i=1}^n \frac{\kappa_i}{\epsilon}$ ,  $m \leftarrow 1$ ,  $\ell \leftarrow 1$ ,  $\tilde{d}_i \leftarrow \epsilon \forall i$ ,  $\tilde{v}_i \leftarrow 0 \forall i$
  - 2: **while**  $\text{Tr} < \tilde{C}$  **do**
  - 3: Listen to the channels  $\{\text{ch}_{k,i}^d\}_{k,i}$  and  $\{\text{ch}_{k,i}^v\}_{k,i}$ , and wait to receive a pulse
  - 4: **if**  $m$ th pulse arrives through  $\text{ch}_{k_m,i_m}^d$  at time  $t_m$  **then**
  - 5:  $q_m = \phi_d(t_m - \lfloor t_m \rfloor)$
  - 6:  $\text{Tr} \leftarrow \text{Tr} - \frac{\kappa_{i_m}(\Delta_{i_m}^{k_m} + q_m)}{\tilde{d}_{i_m}(\tilde{d}_{i_m} + \Delta_{i_m}^{k_m} + q_m)}$
  - 7:  $\tilde{d}_{i_m} = \tilde{d}_{i_m} + \Delta_{i_m}^{k_m} + q_m$
  - 8:  $m \leftarrow m + 1$
  - 9: **end if**
  - 10: **if**  $\ell$ th pulse  $b_\ell$  arrives through  $\text{ch}_{p_\ell,j_\ell}^v$  at time  $p_\ell$  **then**
  - 11:  $\eta_\ell = \phi_v(p_\ell - \lfloor p_\ell \rfloor)$
  - 12:  $\tilde{v}_{j_\ell} = \tilde{v}_{j_\ell} + b_\ell(\gamma_{j_\ell}^{p_\ell} + \eta_\ell)$
  - 13:  $\ell \leftarrow \ell + 1$
  - 14: **end if**
  - 15: **end while**
  - 16: Stop at time  $\tilde{T} = t_m$
  - 17:  $\tilde{D} = \text{diag}(\tilde{d}_1, \dots, \tilde{d}_n)$ ,  $\tilde{U}^{-1} = \tilde{D}^{-1/2} \mathbf{R}^{-1} \tilde{D}^{-1/2}$ ,  $\tilde{V} = [\tilde{v}_1, \dots, \tilde{v}_n]^T$
  - 18:  $\tilde{X} = \tilde{U}^{-1} \tilde{V}$
  - 19: Instruct sensors to stop
- 

where  $\{\tilde{v}_{t,i}\}_i$  compose the approximation  $\tilde{V}_t = [\tilde{v}_{t,1}, \dots, \tilde{v}_{t,n}]^T$ . Recall that the FC employs  $\tilde{V}_t$  to compute the estimator as in (32).

The level-triggered sampling procedure at each sensor  $k$  for each dimension  $i$  is summarized in Algorithm 4. Each sensor  $k$  runs  $n$  of these procedures in parallel. The sequential estimation procedure at the FC is also summarized in Algorithm 5. We assumed, for the sake of clarity, that each sensor transmits pulses to the FC for each dimension through a separate channel, i.e., parallel architecture. On the other hand, in practice the number of parallel channels can be decreased to two by using identical sampling thresholds  $\Delta$  and  $\gamma$  for all sensors and for all dimensions in (33) and (41), respectively. Moreover, sensors can even employ a single channel to convey information about local processes  $\{d_{t,i}^k\}$  and  $\{\bar{v}_{t,i}^k\}$  by sending ternary digits to the FC. This is possible since pulses transmitted for  $\{d_{t,i}^k\}$  are unsigned.

### C. Discussions

We introduced the distributed estimator in Section IV-B initially for a continuous-time system with infinite precision. In practice, due to bandwidth constraints, discrete-time systems with finite precision are of interest. For example, in such systems, the overshoot  $q_{m,i}^k \in [j \frac{\theta_d}{N}, (j+1) \frac{\theta_d}{N})$ ,  $j = 0, 1, \dots, N-1$ ,

is quantized into  $\hat{q}_{m,i}^k = (j + \frac{1}{2}) \frac{\theta}{N}$  where  $N$  is the number of quantization levels. More specifically, a pulse is transmitted at time  $t_{m,i}^k = s_{m,i}^k + \frac{j+1/2}{N}$ , where the transmission delay  $\frac{j+1/2}{N} \in (0, 1)$  encodes  $\hat{q}_{m,i}^k$ . This transmission scheme is called pulse position modulation (PPM).

In UWB and optical communication systems, PPM is effectively employed. In such systems,  $N$ , which denotes the precision, can be easily made large enough so that the quantization error  $|\hat{q}_{m,i}^k - q_{m,i}^k|$  becomes insignificant. Compared to conventional transmission techniques which convey information by varying the power level, frequency, and/or phase of a sinusoidal wave, PPM (with UWB) is extremely energy efficient at the expense of high bandwidth usage. Hence, PPM suits well to energy-constrained sensor network systems.

#### D. Simulation Results

We next provide simulation results to compare the performances of the proposed scheme with linear complexity, given in Algorithm 4 and Algorithm 5, the unsimplified version of the proposed scheme with quadratic complexity and the optimal centralized scheme. A wireless sensor network with 10 identical sensors and an FC is considered to estimate a five-dimensional deterministic vector of parameters, i.e.,  $n = 5$ . We assume i.i.d. Gaussian noise with unit variance at all sensors, i.e.,  $w_t^k \sim \mathcal{N}(0, 1), \forall k, t$ . We set the correlation coefficients  $\{r_{ij}\}$  [cf. (63)] of the vector  $H_t^k$  to different values in  $[0, 1)$ . In Fig. 5 and Fig. 6, they are set to 0 and 0.5 to test the performance of the proposed scheme in the uncorrelated and correlated cases, respectively. We compare the average stopping time performance of the proposed scheme with linear complexity to those of the other two schemes for different MSE values. In Fig. 5 and Fig. 6, the horizontal axis represents the MSE normalized by the square of the Euclidean norm of the vector to be estimated, i.e.,  $\text{nMSE} \triangleq \frac{\text{MSE}}{\|X\|_2^2}$ .

In the uncorrelated case, where  $r_{ij} = 0, \forall i, j, i \neq j$ , the proposed scheme with linear complexity nearly attains the performance of the unsimplified scheme with quadratic complexity as seen in Fig. 5. This result is rather expected since in this case  $\bar{U}_t \cong D_t$  for sufficiently large  $t$ , where  $\bar{U}_t$  and  $D_t$  are used to compute the stopping time and the estimator in the unsimplified and simplified schemes, respectively. Strikingly the distributed schemes (simplified and unsimplified) achieve very close performances to that of the optimal centralized scheme, which is obviously unattainable in a distributed system, thanks to the efficient information transmission through level-triggered sampling. It is seen in Fig. 6 that the proposed simplified scheme exhibits an average stopping time performance close to those of the unsimplified scheme and the optimal centralized scheme even when the scaling coefficients  $\{h_{t,i}^k\}_i$  are correlated with  $r_{ij} = 0.5, \forall i, j, i \neq j$ , justifying the simplification proposed in Section IV-A to obtain linear complexity.

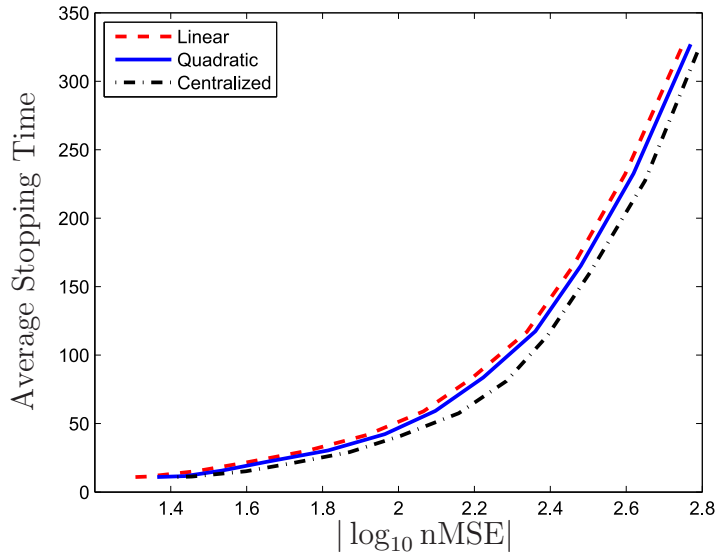


Fig. 5. Average stopping time performances of the optimal centralized scheme and the distributed schemes based on level-triggered sampling with quadratic and linear complexity vs. normalized MSE values when scaling coefficients are uncorrelated, i.e.,  $r_{ij} = 0, \forall i, j$ .

Finally, in Fig. 7 we fix the normalized MSE value at  $10^{-2}$  and plot average stopping time against the correlation coefficient  $r$  where  $r_{ij} = r, \forall i, j, i \neq j$ . We observe an exponential growth in average stopping time of each scheme as  $r$  increases. The average stopping time of each scheme becomes infinite at  $r = 1$  since in this case only some multiples of a certain linear combination of the parameters to be estimated, i.e.,  $h_{t,1}^k \sum_{i=1}^n c_i x_i$ , are observed under the noise  $w_t^k$  at each sensor  $k$  at each time  $t$ , hence it is not possible to recover the individual parameters. Specifically, it can be shown that  $c_i = \sqrt{\frac{\mathbb{E}[(h_{t,i}^k)^2]}{\mathbb{E}[(h_{t,1}^k)^2]}}$ , which is the same for all sensors as we assume identical sensors. To see the mechanism that causes the exponential growth consider the computation of  $\text{Tr}(\bar{\mathbf{U}}_t^{-1})$ , which is used to determine the stopping time in the optimal centralized scheme. From (30) we write

$$\text{Tr}(\bar{\mathbf{U}}_t^{-1}) \cong \text{Tr}(\mathbf{D}_t^{-1} \mathbf{R}^{-1}) = \sum_{i=1}^n \frac{\kappa_i}{d_{t,i}} \quad (44)$$

for sufficiently large  $t$ , where  $d_{t,i}$  and  $\kappa_i$  are the  $i$ th diagonal elements of the matrices  $\mathbf{D}_t$  and  $\mathbf{R}^{-1}$ , respectively. For instance, we have  $\kappa_i = 1, \forall i$ ,  $\kappa_i = 8.0435, \forall i$  and  $\kappa_i = \infty$  when  $r = 0$ ,  $r = 0.9$  and  $r = 1$ , respectively. Assuming that the scaling coefficients have the same mean and variance when  $r = 0$  and  $r = 0.9$ , we have similar  $d_{t,i}$  values [cf. (28)] in (44), hence the stopping time of  $r = 0.9$  is

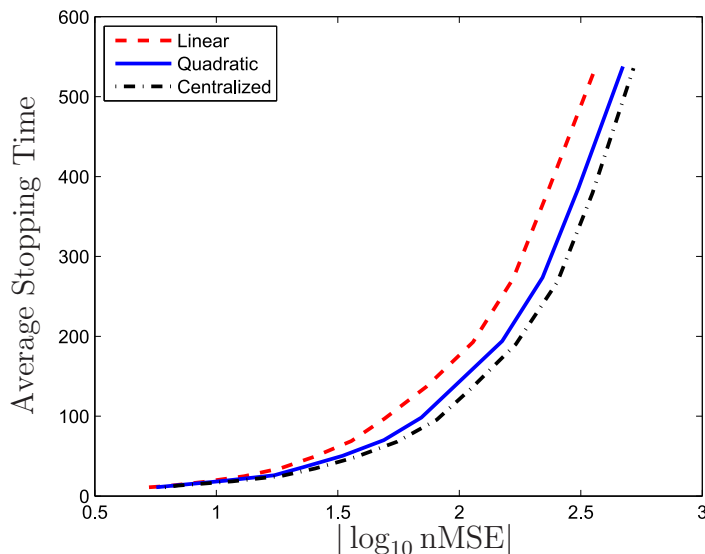


Fig. 6. Average stopping time performances of the optimal centralized scheme and the distributed schemes based on level-triggered sampling with quadratic and linear complexity vs. normalized MSE values when scaling coefficients are correlated with  $r_{ij} = 0.5, \forall i, j$ .

approximately 8 times that of  $r = 0$  for the same accuracy level. Since  $\text{MSE} = \mathbb{E}[\|\hat{X}_{\mathcal{T}} - X\|_2^2] = \text{Tr}(\bar{U}_t^{-1})$  in the centralized scheme, using  $\kappa_i$  for different  $r$  values we can approximately know how the average stopping time changes as  $r$  increases for a given MSE value. As shown in Fig. 7 with the label “Theory” this theoretical curve is in a good match with the numerical result. The small discrepancy at high  $r$  values is due to the high sensitivity of the WLS estimator in (26) to numerical errors when the stopping time is large. The high sensitivity is due to multiplying the matrix  $\bar{U}_{\mathcal{T}}^{-1}$  with very small entries by the vector  $\bar{V}_{\mathcal{T}}$  with very large entries while computing the estimator  $\hat{X}_{\mathcal{T}}$  in (26) for a large  $\mathcal{T}$ . The distributed schemes suffer from a similar high sensitivity problem [cf. (32)] much more than the centralized scheme since making error is inherent in a distributed system. Moreover, in the distributed schemes the MSE is not given by the stopping time statistic  $\text{Tr}(\tilde{U}_t^{-1})$ , hence “Theory” does not match well the curves for the distributed schemes. Although it cannot be used to estimate the rates of the exponential growths of the distributed schemes, it is still useful to explain the mechanism behind them as the distributed schemes are derived from the centralized scheme.

To summarize, with identical sensors any estimator (centralized or distributed) experiences an exponential growth in its average stopping time as the correlation between scaling coefficients increases since in the extreme case of full correlation, i.e.,  $r = 1$ , each sensor  $k$ , at each time  $t$ , observes a noisy

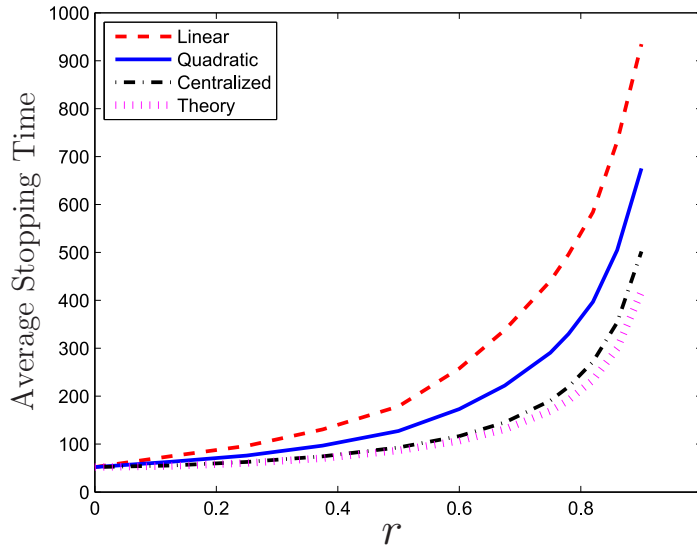


Fig. 7. Average stopping time performances of the optimal centralized scheme and the distributed schemes based on level-triggered sampling with quadratic and linear complexity vs. correlation coefficient for normalized MSE fixed to  $10^{-2}$ .

sample of the linear combination  $\sum_{i=1}^n x_i \sqrt{\frac{\mathbb{E}[(h_{t,i}^k)^2]}{\mathbb{E}[(h_{t,1}^k)^2]}}$ , and thus the stopping time is infinite. As a result of exponentially growing stopping time, the WLS estimator, which is also the ML estimator and the MVUE, i.e., the optimal estimator, in our case, and the distributed estimators derived from it become highly sensitive to errors as  $r$  increases. In either uncorrelated or mildly correlated cases, which are of practical importance, the proposed distributed scheme with linear complexity performs very close to the optimal centralized scheme as shown in Fig. 5 and Fig. 6, respectively.

## V. CONCLUSIONS

We have treated the problem of sequential vector parameter estimation under both centralized and distributed settings. In the centralized setting two different formulations, which use unconditional and conditional covariances of the estimator respectively to assess the estimation accuracy, are considered and the corresponding sequential estimators are derived. The conditional formulation, having a simple stopping rule for any number of parameters, was shown to be preferable to the unconditional formulation, whose stopping rule can only be found by complicated numerical computations even for a small number of parameters. Moreover, following the optimal conditional sequential estimator we have developed a computationally efficient distributed sequential estimator based on level-triggered sampling. Simulation

results have shown that the proposed scheme with linear complexity has a similar performance to that of the optimal centralized scheme.

#### APPENDIX A: PROOF OF LEMMA 1

In the Section II, the LS estimator was shown to be the MVUE under Gaussian noise and the BLUE under non-Gaussian noise. It was also shown that  $\text{Cov}(\hat{X}_t|\mathbf{H}_t) = \sigma^2\mathbf{U}_t^{-1}$ . Hence, we write

$$\begin{aligned} f\left(\text{Cov}(\hat{X}_{\mathcal{T}}|\mathbf{H}_{\mathcal{T}})\right) &= f\left(\mathbb{E}\left[\sum_{t=1}^{\infty}(\hat{X}_t - X)(\hat{X}_t - X)^T \mathbb{1}_{\{t=\mathcal{T}\}}|\mathbf{H}_{\mathcal{T}}\right]\right) \\ &= f\left(\sum_{t=1}^{\infty}\mathbb{E}\left[(\hat{X}_t - X)(\hat{X}_t - X)^T|\mathbf{H}_t\right] \mathbb{1}_{\{t=\mathcal{T}\}}\right) \end{aligned} \quad (45)$$

$$\geq f\left(\sum_{t=1}^{\infty}\sigma^2\mathbf{U}_t^{-1} \mathbb{1}_{\{t=\mathcal{T}\}}\right) \quad (46)$$

$$= f(\sigma^2\mathbf{U}_{\mathcal{T}}^{-1}), \quad (47)$$

for all unbiased estimators under Gaussian noise and for all linear unbiased estimators under non-Gaussian noise. The indicator function  $\mathbb{1}_{\{A\}} = 1$  if  $A$  is true, and 0 otherwise. We used the facts that the event  $\{\mathcal{T} = t\}$  is  $\mathcal{H}_t$ -measurable and  $\mathbb{E}[(\hat{X}_t - X)(\hat{X}_t - X)^T|\mathbf{H}_t] = \text{Cov}(\hat{X}_t|\mathbf{H}_t) \geq \sigma^2\mathbf{U}_t^{-1}$  to write (45) and (46), respectively.

#### APPENDIX B: PROOF OF LEMMA 2

We will first prove that if  $\mathcal{V}(z)$  is non-decreasing, concave and bounded, then so is  $G(z) = 1 + \mathbb{E}\left[\mathcal{V}\left(\frac{z}{1+zh_1^2}\right)\right]$ . That is, assume  $\mathcal{V}(z)$  satisfies: (a)  $\frac{d}{dz}\mathcal{V}(z) \geq 0$ , (b)  $\frac{d^2}{dz^2}\mathcal{V}(z) < 0$ , (c)  $\mathcal{V}(z) < c < \infty, \forall z$ . Then by (c) we have

$$1 + \mathcal{V}\left(\frac{z}{1+zh_1^2}\right) < 1 + c, \forall z, \quad (48)$$

hence  $G(z) < 1 + c$  is bounded. Moreover,

$$\frac{d}{dz}\mathcal{V}\left(\frac{z}{1+zh_1^2}\right) = \frac{\frac{d}{dz}\mathcal{V}(z)}{(1+zh_1^2)^2} > 0, \quad \forall z \quad (49)$$

by (a), and thus  $G(z)$  is non-decreasing. Furthermore,

$$\frac{d^2}{dz^2}G(z) = \mathbb{E}\left[\frac{d^2}{dz^2}\mathcal{V}\left(\frac{z}{1+zh_1^2}\right)\right] = \mathbb{E}\left[\underbrace{\frac{\frac{d^2}{dz^2}\mathcal{V}(z)}{(1+zh_1^2)^4}}_{<0 \text{ by (b)}} + \underbrace{\frac{\frac{d}{dz}\mathcal{V}(z)}{-(1+zh_1^2)^3/2h_1^2}}_{<0 \text{ by (a) \& } z=\frac{1}{u}>0}\right], \quad \forall z, \quad (50)$$

hence  $G(z)$  is concave, concluding the first part of the proof.

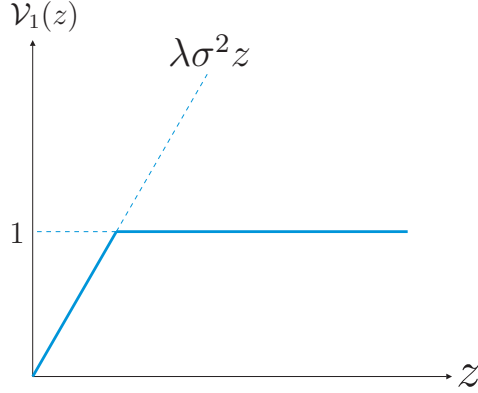


Fig. 8. The function  $\mathcal{V}_1(z)$  is non-decreasing and concave.

Now, it is sufficient to show that  $\mathcal{V}(z)$  is non-decreasing, concave and bounded. Assume that the limit  $\lim_{m \rightarrow \infty} \mathcal{V}_m(z) = \mathcal{V}(z)$  exists. We will prove the existence of the limit later. First, we will show that  $\mathcal{V}(z)$  is non-decreasing and concave by iterating the functions  $\{\mathcal{V}_m(z)\}$ . Start with  $\mathcal{V}_0(z) = 0$ . Then,

$$\mathcal{V}_1(z) = \min \left\{ \lambda \sigma^2 z, 1 + \mathbb{E} \left[ \mathcal{V}_0 \left( \frac{z}{1 + zh_1^2} \right) \right] \right\} = \min \{ \lambda \sigma^2 z, 1 \}, \quad (51)$$

which is non-decreasing and concave as shown in Fig. 8. Similarly we write

$$\mathcal{V}_2(z) = \min \left\{ \lambda \sigma^2 z, 1 + \mathbb{E} \left[ \mathcal{V}_1 \left( \frac{z}{1 + zh_1^2} \right) \right] \right\}, \quad (52)$$

where  $1 + \mathbb{E} \left[ \mathcal{V}_1 \left( \frac{z}{1 + zh_1^2} \right) \right]$  is non-decreasing and concave since  $\mathcal{V}_1(z)$  is non-decreasing and concave. Hence,  $\mathcal{V}_2(z)$  is non-decreasing and concave since pointwise minimum of non-decreasing and concave functions is again non-decreasing and concave. We can show in the same way that  $\mathcal{V}_m(z)$  is non-decreasing and concave for  $m > 2$ , i.e.,  $\mathcal{V}(z) = \mathcal{V}_\infty(z)$  is non-decreasing and concave.

Next, we will show that  $\mathcal{V}(z)$  is bounded. Assume that

$$\mathcal{V}(z) < \min \{ \lambda \sigma^2 z, c \} = \lambda \sigma^2 z \mathbb{1}_{\{ \lambda \sigma^2 z \leq c \}} + c \mathbb{1}_{\{ \lambda \sigma^2 z > c \}}. \quad (53)$$

Then, from the definition of  $\mathcal{V}(z)$  we have  $1 + \mathbb{E} \left[ \mathcal{V} \left( \frac{z}{1 + zh_1^2} \right) \right] < c$ . Since  $\mathcal{V}(z)$  is non-decreasing,  $\mathbb{E} \left[ \mathcal{V} \left( \frac{z}{1 + zh_1^2} \right) \right] \leq \mathbb{E} \left[ \mathcal{V} \left( \frac{1}{h_1^2} \right) \right]$ . From (53) we can write

$$1 + \mathbb{E} \left[ \mathcal{V} \left( \frac{z}{1 + zh_1^2} \right) \right] \leq 1 + \mathbb{E} \left[ \mathcal{V} \left( \frac{1}{h_1^2} \right) \right] < 1 + \mathbb{E} \left[ \frac{\lambda \sigma^2}{h_1^2} \mathbb{1}_{\{ \frac{\lambda \sigma^2}{h_1^2} \leq c \}} \right] + c \mathbb{P} \left( \frac{\lambda \sigma^2}{h_1^2} > c \right), \quad (54)$$

Recalling  $1 + \mathbb{E} \left[ \mathcal{V} \left( \frac{z}{1 + zh_1^2} \right) \right] < c$  we want to find a  $c$  such that

$$1 + \mathbb{E} \left[ \frac{\lambda \sigma^2}{h_1^2} \mathbb{1}_{\{ \frac{\lambda \sigma^2}{h_1^2} \leq c \}} \right] + c \mathbb{P} \left( \frac{\lambda \sigma^2}{h_1^2} > c \right) < c. \quad (55)$$

For such a  $c$  we have

$$\begin{aligned} 1 &< c \mathbb{P}\left(\frac{\lambda\sigma^2}{h_1^2} \leq c\right) - \mathbb{E}\left[\frac{\lambda\sigma^2}{h_1^2} \mathbb{1}_{\{\frac{\lambda\sigma^2}{h_1^2} \leq c\}}\right] \\ &= \mathbb{E}\left[\left(c - \frac{\lambda\sigma^2}{h_1^2}\right) \mathbb{1}_{\{\frac{\lambda\sigma^2}{h_1^2} \leq c\}}\right] = \mathbb{E}\left[\left(c - \frac{\lambda\sigma^2}{h_1^2}\right)^+\right], \end{aligned} \quad (56)$$

where  $(\cdot)^+$  is the positive part operator. We need to show that there exists a  $c$  satisfying  $\mathbb{E}\left[\left(c - \frac{\lambda\sigma^2}{h_1^2}\right)^+\right] >$

1. Note that we can write

$$\begin{aligned} \mathbb{E}\left[\left(c - \frac{\lambda\sigma^2}{h_1^2}\right)^+\right] &\geq \mathbb{E}\left[\left(c - \frac{\lambda\sigma^2}{h_1^2}\right)^+ \mathbb{1}_{\{h_1^2 > \epsilon\}}\right] \\ &> \mathbb{E}\left[\left(c - \frac{\lambda\sigma^2}{\epsilon}\right)^+ \mathbb{1}_{\{h_1^2 > \epsilon\}}\right] \\ &= \left(c - \frac{\lambda\sigma^2}{\epsilon}\right)^+ \mathbb{P}(h_1^2 > \epsilon), \end{aligned} \quad (57)$$

where  $\left(c - \frac{\lambda\sigma^2}{\epsilon}\right)^+ \rightarrow \infty$  as  $c \rightarrow \infty$  since  $\lambda$  and  $\epsilon$  are constants. If  $\mathbb{P}(h_1^2 > \epsilon) > 0$ , which is always true except the trivial case where  $h_1 = 0$  deterministically, then the desired  $c$  exists.

Now, what remains is to justify our initial assumption  $\mathcal{V}(z) < \min\{\lambda\sigma^2 z, c\}$ . We will use induction to show that the assumption holds with the  $c$  found above. From (51), we have  $\mathcal{V}_1(z) = \min\{\lambda\sigma^2 z, 1\} < \min\{\lambda\sigma^2 z, c\}$  since  $c > 1$ . Then, assume that

$$\mathcal{V}_{m-1}(z) < \min\{\lambda\sigma^2 z, c\} = \lambda\sigma^2 z \mathbb{1}_{\{\lambda\sigma^2 z \leq c\}} + c \mathbb{1}_{\{\lambda\sigma^2 z > c\}}. \quad (58)$$

We need to show that  $\mathcal{V}_m(z) < \min\{\lambda\sigma^2 z, c\}$ , where  $\mathcal{V}_m(z) = \min\left\{\lambda\sigma^2 z, 1 + \mathbb{E}\left[\mathcal{V}_{m-1}\left(\frac{z}{1+z h_1^2}\right)\right]\right\}$ . Note that  $1 + \mathbb{E}\left[\mathcal{V}_{m-1}\left(\frac{z}{1+z h_1^2}\right)\right] \leq 1 + \mathbb{E}\left[\mathcal{V}_{m-1}\left(\frac{1}{h_1^2}\right)\right]$  since  $\mathcal{V}_{m-1}(z)$  is non-decreasing. Similar to (54), from (58) we have

$$1 + \mathbb{E}\left[\mathcal{V}_{m-1}\left(\frac{1}{h_1^2}\right)\right] < 1 + \mathbb{E}\left[\frac{\lambda\sigma^2}{h_1^2} \mathbb{1}_{\{\frac{\lambda\sigma^2}{h_1^2} \leq c\}}\right] + c \mathbb{P}\left(\frac{\lambda\sigma^2}{h_1^2} > c\right) < c, \quad (59)$$

where the last inequality follows from (55). Hence,

$$\mathcal{V}_m(z) < \min\{\lambda\sigma^2 z, c\}, \quad \forall m, \quad (60)$$

showing that  $\mathcal{V}(z) < \min\{\lambda\sigma^2 z, c\}$ , which is the assumption in (53).

We showed that  $\mathcal{V}(z)$  is non-decreasing, concave and bounded if it exists, i.e., the limit  $\lim_{m \rightarrow \infty} \mathcal{V}_m(z)$  exists. Note that we showed in (60) that the sequence  $\{\mathcal{V}_m\}$  is bounded. If we also show that  $\{\mathcal{V}_m\}$  is monotonic, e.g., non-decreasing, then  $\{\mathcal{V}_m\}$  converges to a finite limit  $\mathcal{V}(z)$ . We will again use induction to show the monotonicity for  $\{\mathcal{V}_m\}$ . From (51) we write  $\mathcal{V}_1(z) = \min\{\lambda\sigma^2 z, 1\} \geq \mathcal{V}_0(z) = 0$ . Assuming

$\mathcal{V}_{m-1}(z) \geq \mathcal{V}_{m-2}(z)$  we need to show that  $\mathcal{V}_m(z) \geq \mathcal{V}_{m-1}(z)$ . Using their definitions we write  $\mathcal{V}_m(z) = \min \left\{ \lambda \sigma^2 z, 1 + \mathbb{E} \left[ \mathcal{V}_{m-1} \left( \frac{z}{1+z h_1^2} \right) \right] \right\}$  and  $\mathcal{V}_{m-1}(z) = \min \left\{ \lambda \sigma^2 z, 1 + \mathbb{E} \left[ \mathcal{V}_{m-2} \left( \frac{z}{1+z h_1^2} \right) \right] \right\}$ . We have  $1 + \mathbb{E} \left[ \mathcal{V}_{m-1} \left( \frac{z}{1+z h_1^2} \right) \right] \geq 1 + \mathbb{E} \left[ \mathcal{V}_{m-2} \left( \frac{z}{1+z h_1^2} \right) \right]$  due to the assumption  $\mathcal{V}_{m-1}(z) \geq \mathcal{V}_{m-2}(z)$ , hence  $\mathcal{V}_m(z) \geq \mathcal{V}_{m-1}(z)$ .

To conclude, we proved that  $\mathcal{V}_m(z)$  is non-decreasing and bounded in  $m$ , thus the limit  $\mathcal{V}(z)$  exists, which was also shown to be non-decreasing, concave and bounded. Hence,  $G(z)$  is non-decreasing, concave and bounded.

### APPENDIX C: PROOF OF PROPOSITION 1

The simplified distributed scheme that we propose in Section IV is motivated from the special case where  $\mathbb{E}[h_{t,i}^k h_{t,j}^k] = 0$ ,  $\forall k, i, j = 1, \dots, n, i \neq j$ . In this case, by the *law of large numbers* for sufficiently large  $t$  the off-diagonal elements of  $\bar{\mathbf{U}}_t$  vanish, and thus we have  $\bar{\mathbf{U}}_t \cong \mathbf{D}_t$  and  $\text{Tr}(\bar{\mathbf{U}}_t^{-1}) \cong \text{Tr}(\mathbf{D}_t^{-1})$ . For the general case where we might have  $\mathbb{E}[h_{t,i}^k h_{t,j}^k] \neq 0$  for some  $k$  and  $i \neq j$ , using the diagonal matrix  $\mathbf{D}_t$  we write

$$\text{Tr}(\bar{\mathbf{U}}_t^{-1}) = \text{Tr} \left( \left( \mathbf{D}_t^{1/2} \underbrace{\mathbf{D}_t^{-1/2} \bar{\mathbf{U}}_t \mathbf{D}_t^{-1/2}}_{\mathbf{R}_t} \mathbf{D}_t^{1/2} \right)^{-1} \right) \quad (61)$$

$$\begin{aligned} &= \text{Tr} \left( \mathbf{D}_t^{-1/2} \mathbf{R}_t^{-1} \mathbf{D}_t^{-1/2} \right) \\ &= \text{Tr} \left( \mathbf{D}_t^{-1} \mathbf{R}_t^{-1} \right). \end{aligned} \quad (62)$$

Note that each entry  $r_{t,ij}$  of the newly defined matrix  $\mathbf{R}_t$  is a normalized version of the corresponding entry  $\bar{u}_{t,ij}$  of  $\bar{\mathbf{U}}_t$ . Specifically,  $r_{t,ij} = \frac{\bar{u}_{t,ij}}{\sqrt{d_{t,i} d_{t,j}}} = \frac{\bar{u}_{t,ij}}{\sqrt{u_{t,ii} u_{t,jj}}}$ ,  $i, j = 1, \dots, n$ , where the last equality follows from the definition of  $d_{t,i}$  in (28). Hence,  $\mathbf{R}_t$  has the same structure as in (29) with entries

$$r_{t,ij} = \frac{\sum_{k=1}^K \sum_{p=1}^t \frac{h_{p,i}^k h_{p,j}^k}{\sigma_k^2}}{\sqrt{\sum_{k=1}^K \sum_{p=1}^t \frac{(h_{p,i}^k)^2}{\sigma_k^2} \sum_{k=1}^K \sum_{p=1}^t \frac{(h_{p,j}^k)^2}{\sigma_k^2}}}, \quad i, j = 1, \dots, n.$$

For sufficiently large  $t$ , by the law of large numbers

$$r_{t,ij} \cong r_{ij} = \frac{\sum_{k=1}^K \frac{\mathbb{E}[h_{t,i}^k h_{t,j}^k]}{\sigma_k^2}}{\sqrt{\sum_{k=1}^K \frac{\mathbb{E}[(h_{t,i}^k)^2]}{\sigma_k^2} \sum_{k=1}^K \frac{\mathbb{E}[(h_{t,j}^k)^2]}{\sigma_k^2}}} \quad (63)$$

and  $\mathbf{R}_t \cong \mathbf{R}$ , where  $\mathbf{R}$  is given in (29). Hence, for sufficiently large  $t$  we can make the approximations in (30) using (61) and (62).

## REFERENCES

- [1] Y. Yilmaz, and X. Wang, “Sequential Decentralized Parameter Estimation under Randomly Observed Fisher Information,” *IEEE Trans. Inf. Theory*, to be published
- [2] B. Efron, and D.V. Hinkley, “Assessing the accuracy of the maximum likelihood estimator: Observed versus expected Fisher information,” *Biometrika*, vol. 65, no. 3, pp. 457-487, 1978.
- [3] P. Grambsch, “Sequential sampling based on the observed Fisher information to guarantee the accuracy of the maximum likelihood estimator,” *Ann. Statist.*, vol. 11, no. 1, pp. 68–77, 1983.
- [4] G. Fellouris, “Asymptotically optimal parameter estimation under communication constraints,” *Ann. Statist.*, vol. 40, no. 4, pp. 2239–2265, Aug. 2012
- [5] Y. Yilmaz, G.V. Moustakides, and X. Wang, “Cooperative sequential spectrum sensing based on level-triggered sampling,” *IEEE Trans. Signal Process.*, vol. 60, no. 9, pp. 4509–4524, Sept. 2012.
- [6] G. Fellouris and G.V. Moustakides, “Decentralized sequential hypothesis testing using asynchronous communication,” *IEEE Trans. Inf. Theory*, vol. 57, no. 1, pp. 534-548, Jan. 2011.
- [7] Y. Yilmaz, G.V. Moustakides, and X. Wang, “Channel-aware decentralized detection via level-triggered sampling,” *IEEE Trans. Signal Process.*, vol. 61, no. 1, pp. 300–315, Jan. 2013.
- [8] B.K. Ghosh, “On the attainment of the Cramér-Rao bound in the sequential case,” *Sequential Analysis*, vol. 6, no. 3, pp. 267–288, 1987.
- [9] A. Ribeiro, and G.B. Giannakis, “Bandwidth-Constrained Distributed Estimation for Wireless Sensor Networks Part II: Unknown Probability Density Function,” *IEEE Trans. Signal Process.*, vol. 54, no. 7, pp. 2784–2796, July 2006.
- [10] E.J. Msechu, and G.B. Giannakis, “Sensor-Centric Data Reduction for Estimation With WSNs via Censoring and Quantization,” *IEEE Trans. Signal Process.*, vol. 60, no. 1, pp. 400–414, Jan. 2012.
- [11] J.J. Xiao, A. Ribeiro, Z.Q. Luo, and G.B. Giannakis, “Distributed Compression-Estimation Using Wireless Sensor Networks,” *IEEE Signal Process. Mag.*, vol. 23, no. 4, pp. 27–41, July 2006.
- [12] J.J. Xiao, S. Cui, Z.Q. Luo, and A.J. Goldsmith, “Linear Coherent Decentralized Estimation,” *IEEE Trans. Signal Process.*, vol. 56, no. 2, pp. 757–770, Feb. 2008.
- [13] Z.Q. Luo, G.B. Giannakis, and S. Zhang, “Optimal Linear Decentralized Estimation in a Bandwidth Constrained Sensor Network,” in Proc. 2005 IEEE Int. Symp. Inform. Theory (ISIT’05), pp. 1441–1445, Sept. 2005.
- [14] I.D. Schizas, G.B. Giannakis, and Z.Q. Luo, “Distributed Estimation Using Reduced-Dimensionality Sensor Observations,” *IEEE Trans. Signal Process.*, vol. 55, no. 8, pp. 4284–4299, Aug. 2007.
- [15] I.D. Schizas, A. Ribeiro, and G.B. Giannakis, “Consensus in Ad Hoc WSNs With Noisy Links-Part I: Distributed Estimation of Deterministic Signals,” *IEEE Trans. Signal Process.*, vol. 56, no. 1, pp. 350–364, Jan. 2008.
- [16] S.S. Stankovic, M.S. Stankovic, and D.M. Stipanovic, “Decentralized Parameter Estimation by Consensus Based Stochastic Approximation,” *IEEE Trans. Autom. Control*, vol. 56, no. 3, pp. 531–543, Mar. 2011.
- [17] V. Borkar, and P.P. Varaiya, “Asymptotic Agreement in Distributed Estimation,” *IEEE Trans. Autom. Control*, vol. 27, no. 3, pp. 650–655, June 1982.
- [18] T. Zhao, and A. Nehorai, “Distributed Sequential Bayesian Estimation of a Diffusive Source in Wireless Sensor Networks,” *IEEE Trans. Signal Process.*, vol. 55, no. 4, pp. 1511–1524, Apr. 2007.
- [19] A.N. Shiryaev, *Optimal Stopping Rules*, Springer, New York, 2008.
- [20] T. Vercauteren, and X. Wang, “Decentralized Sigma-Point Information Filters for Target Tracking in Collaborative Sensor Networks,” *IEEE Trans. Signal Process.*, vol. 53, no. 8, pp. 2997–3009, Aug. 2005.